

MACK, TODD STEVEN, M.S. Regulation of Cytochrome P450 2A6 and Phase II Enzymes by Unsaturated Aldehydes. (2009)
Directed by Dr. Gregory M. Raner. 57 pp.

Human Phase I and Phase II drug metabolizing enzymes are known to interact with foreign chemicals that enter the body as a defense mechanism, however, it is often the case that unwanted interactions can occur. Phase I metabolism may form reactive electrophiles that can covalently modify DNA, proteins and lipids. These modified electrophilic biomolecules are thought to cause progression of many diseases such as Parkinson's and Alzheimer's Disease (3). On the other hand, Phase II enzymes can remove the toxic compounds of the Phase I enzymes. The Phase II enzymes are likely induced via biochemical pathway involving the nuclear transcription factor Nrf2 (4).

This current study was designed to probe specific interactions between commonly used essential oils, along with their major aldehyde constituents, and CYP2A6. The overall goal was to gain a better understanding of factors that may govern the inhibitory effects of aldehydes on this isoform. In addition, the ability of the essential oil of Cassia and its primary constituent, cinnamaldehyde on Phase II gene induction was probed as well using cultured human hepatoma cells (HepG2). Here the goal was to gain a better understanding of the relationship between oxidative stress, and aldehydes that may be present in commonly used products. The results demonstrated that relatively small unsaturated aldehydes (6-8 carbons) showed a dramatic decrease in the CYP2A6 activity when catalyzing the coumarin 7-hydroxylation reaction. This inhibition could translate to a net antioxidant effect, by preventing the formation of reactive oxygen species (ROS), particularly in the presence of 2A6-activated nitrosamines, which can be carcinogenic. It

was also shown that Cassia and cinnamaldehyde had an inductive effect on Phase II enzymes in human hepatoma cells, such as heme oxygenase 1 (HO1) and epoxide hydrolase (EPHX), thus exerting a net anti-oxidant effect on the cells as a whole.

REGULATION OF CYTOCHROME P450 2A6 AND
PHASE II ENZYMES BY UNSATURATED
ALDEHYDES.

by

Todd Steven Mack

A Thesis Submitted to
The Faculty of The Graduate School at
The University of North Carolina at Greensboro
in Partial Fulfillment
of the Requirements for the Degree
Master of Science

Greensboro
2009

Approved by

Committee Chair

To my Mother and Father,
Without your encouragement this would not have been possible,
and to Maria,
Thank you for you love and support.

APPROVAL PAGE

This thesis has been approved by the following committee of the Faculty of The Graduate School at The University of North Carolina at Greensboro.

Committee Chair _____

Committee Members _____

Date of Acceptance by Committee

Date of Final Oral Examination

ACKNOWLEDGEMENTS

I would first like to thank Dr. Greg Raner for his guidance and financial support through my graduate work at UNCG. I would also like to acknowledge Dr. Nadja Cech for her assistance through my graduate work. Finally, I would like to thank Dr. Bruce Banks for his guidance through my graduate work.

TABLE OF CONTENTS

	Page
LIST OF TABLES	vii
LIST OF FIGURES	viii
CHAPTER	
I. INTRODUCTION	1
I. A. Phase I Enzyme- Cytochrome P450.....	2
I. B. Cytochrome P450 2A6.....	4
I. B. i. CYP2A6-Active Site.....	5
I. B. ii. CYP2A6-Role in Nicotine Metabolism.....	6
I. B. iii. Smoking and CYP2A6 Role on Cancer Risk	7
I. C. 2A6 Potential Inhibitors.....	8
I. D. Phase II Enzymes- Anti-Oxidant Response.....	9
I. E. Balance of Phase I and Phase II Enzymes.....	13
II. MATERIALS AND METHODS	14
II. A. CYP 2A6 Inhibition Screening Method.....	14
II. A. i. HPLC Analysis.....	15
II. A. ii. K _i Determination	15
II. B. HepG2- Cell Culturing.....	17
II. C. HepG2- Phase II Enzyme Induction.	18
II. D. Total RNA Isolation and Purification.....	21
II. E. RT-PCR of Purified RNA Samples	23
II. F. Gel Agarose.....	24
III. RESULTS AND DISCUSSION.....	26
III. A. Inhibition of CYP2A6 by various.....	26
III. A. i. Essential Oils Inhibition Analysis	28
III. A. ii. Individual Aldehyde Effects on CYP2A6.....	30
III. B. Inductions of Phase II Drug Metabolizing Enzymes by Essential Oils and Aldehydes.....	45
III. B. i. RT-PCR Internal Controls: β-actin and GAPDH.....	46
III. B. ii. RT-PCR Analysis of EPHX1.....	47
III. B. iii. RT-PCR Analysis of HNMT	47

III. B. iv. RT-PCR Analysis of HAT1.....	48
III. B. v. RT-PCR Analysis of Heme Oxygenase-1	49
IV. CONCLUSIONS.....	54
REFERENCES	56

LIST OF TABLES

	Page
II. 1: List of primer sequences, product size and annealing temperature used to show Phase II enzymes induction.....	24
III. 1: Values of V_{\max} and $V_{\max \text{ app}}$ from the Michaelis-Menton Plots for each aldehyde.....	45
III. 2: Calculated values for K_I , K_M , $K_{M \text{ app}}$ for each Unsaturated Aldehyde as listed.....	45

LIST OF FIGURES

	Page
I. 1: Coumarin 7-hydroxylation is catalyzed by CYP2A6.....	4
I. 2: Structure of CYP2A6 with coumarin bound to the active site showing Phe 107 π stacking interactions, and Asn 297 H-bonding to the oxygen on the substrate (10).....	6
I. 3: Metabolism Pathway of Nicotine into Cotinine.....	7
I. 4: General overview of the mechanism in which the electrophile (oxidant) initiates the Nrf2 system.....	11
II.1: Experimental setup for dose dependent studies probing for the induction of Phase II enzymes in HepG2 cells.....	20
II.2: Experimental setup for time dependent studies probing for the induction of Phase II enzymes in HepG2 cells.....	21
III. 1: 7-Hydroxycoumarin standard HPLC chromatogram containing 7-hydroxycoumarin.....	27
III. 2: A sample of a HPLC chromatogram obtained with the 7-hydroxylation assay.....	28
III. 3: Plot of percent activity of CYP2A6 using human liver microsomes	30
III. 4: Screening of Aromatic Aldehydes, benzaldehyde and cinnamaldehyde	32
III. 5: Plot of area vs. coumarin concentration in the presence (red) and absence (green) of trans-cinnamaldehyde (0.0605 mM).....	34
III. 6: A reaction probing for the activity of CYP2A6 used a broad range of inhibitors (saturated aldehydes and carboxylic acid).....	36
III. 7: A reaction probing for the activity of CYP2A6 used a broad range of inhibitors (unsaturated aldehydes).....	37

III. 8: Plot of area vs. coumarin concentration in the presence (red) and absence (green) of crotonaldehyde (0.557 mM).....	40
III. 9: Plot of area vs. coumarin concentration in the presence (red) and absence (green) of trans-2-pentenal (0.464 mM).....	41
III. 10: Plot of area vs. coumarin concentration in the presence (red) and absence (green) of trans-2-hexenal (0.133 mM).....	42
III. 11: Plot of area vs. coumarin concentration in the presence (red) and absence (green) of trans-2-octenal (0.0754 mM).....	43
III. 12: Plot of area vs. coumarin concentration in the presence (red) and absence (green) of trans-2-nonenal (0.125 mM).....	44
III. 13: Gel electrophoresis of the β -actin gene showed a constant band for all of the samples.....	49
III. 14: Gel Electrophoresis of the induction of the HO-1 gene in HepG2 cells, in the presence of increasing concentrations of cassia essential oil from 0.01 μ g/mL to 0.10 μ g/mL, with a five hour incubation at 37°C.....	52
III. 15: Gel Electrophoresis of the induction of the HO-1 gene in HepG2 cells, in the presence of 0.02 μ g/mL cassia oil for 0, 1, 6, and 24 hours of incubation at 37°C.....	52
III. 16: Gel Electrophoresis of the induction of the HO-1 gene in HepG2 cells, in the presence of increasing concentrations of cinnamaldehyde from 0.01 μ g/mL to 0.10 μ g/mL, with a five hour incubation at 37°C	53
III. 17: Gel Electrophoresis of the induction of the HO-1 gene in HepG2 cells, in the presence of 0.02 μ g/mL cinnamaldehyde for 0, 1, 6, and 24 hours of incubation at 37°C.....	53

CHAPTER I

INTRODUCTION

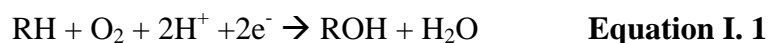
Cellular oxidative metabolism, including drug and xenobiotic biotransformations, may form reactive electrophiles that can covalently modify DNA, proteins and lipids. These modified electrophilic biomolecules are thought to cause progression of many diseases (2). The ultimate goal is to gain a better understanding of the relationship that between Reactive Oxygen Species (ROS) and the body's defense system against foreign chemicals, namely Phase I and Phase II drug metabolism. Controlling ROS levels is a key to preventing and/or controlling the progression of many life threatening diseases. The metabolic pathways that remove foreign chemicals (xenobiotics), along with aerobic metabolism itself, can generate ROS or other oxidized chemicals that can cause cellular damage. These xenobiotics and ROS are eliminated from the body by a multi-step pathway involving drug metabolism enzymes. Drug metabolism enzymes are classified as either Phase I, II, or III. Phase I enzymes are involved in the oxidation of xenobiotics, such as Cytochrome P450s. Phase II enzymes deal with the activated compounds that Phase I enzymes created by converting them into hydrophilic conjugates facilitating their removal (detoxification). Phase III enzymes are involved in eliminating the Phase II metabolites from the cells. (3)

The goal of this work was to gain a better understanding of the involvement of drug metabolizing enzymes, Phase I and Phase II enzymes, and the effects that essential

oils, and aldehydes have on the activity of these enzymes. The initial focus was on essential oils and various aldehydes that may possess antioxidant properties, by preventing the formation of reactive oxygen species (ROS). These oils/aldehydes were used to probe the inhibition of human Cytochrome P450_{2A6} in human liver microsomes by utilization of the unique ability of 2A6 to catalyze the conversion of coumarin to 7-hydroxycoumarin. Next, induction of Phase II anti-oxidant genes in cultured human hepatoma (HepG2) cells by oils and purified aldehydes was monitored using RT-PCR in order to assess the potential of these natural products to induce the expression of antioxidant enzymes.

I. A. Phase I Enzyme- Cytochrome P450

Cytochrome P450 (CYP) is the most common Phase I enzyme responsible for the oxidative metabolism of xenobiotics found in foods, beverages, tobacco products, cosmetics, natural products and the majority of drugs on the market today (4). This is a very diverse superfamily of hemoproteins found in many different species ranging from mammals to archaea (4). These proteins are located all over the body but the majority of them are located within the liver. The most common reaction that cytochrome P450s catalyze is a monooxygenase reaction in which a substrate gets one oxygen from molecular oxygen incorporated into it and the other oxygen forms water as shown below in **Equation I. 1** (4).



Cytochrome P450 are typically abbreviated CYP. The many different subfamilies have specific nomenclature that go along with it as well, such as CYP2A6. The

nomenclature is based on gene family, which is indicated by a Arabic numeral following the CYP abbreviation, a capital letter follows, indicating the subfamily, followed by another number for the which particular gene it is. The active site of the enzyme contains a heme iron center that takes part in catalysis (4).

Cytochrome P450s in humans are of great interest because of their ability to metabolize a broad range of endogenous and exogenous compounds. In the liver, the types of the compounds that are metabolized include drugs and a variety of other environmental chemicals. In the other areas of the body where cytochrome P450s reside, they are involved in a great variety of functions. They are used for hormone synthesis and breakdown, cholesterol synthesis, and vitamin D metabolism (2).

CYPs within the liver account for about 75% of drug metabolism and bio-activation. Some drugs may act to inhibit or increase specific CYP activity, thereby increasing the potential to interact with other drugs. These interactions can have significant consequences for patients when taking certain drugs together (4). There are many compounds, other than drugs, that can induce or inhibit CYP activity. Natural products found in grapefruit juice for example, are well known inhibitors of CYP3A4 and it is therefore usually advised that patients avoid drinking grapefruit juice all together when taking any medication. Other products that have been shown to interact with major CYPs are Saint John's Wort, which induces CYP3A4, tobacco smoking which induces CYP1A2, and starfruit juice which inhibits CYP2A6 (4).

The induction of Phase I enzymes has been shown to be mediated via a diverse set of nuclear receptors that activate the transcription of these enzymes. These receptors

include aryl hydrocarbon receptor (AhR), halogenated aromatic hydrocarbon receptor, and also receptors for many steroid-like compounds (6). The AhRs are primarily receptors that respond to xenobiotics that enter the body, and their response elements are the xenobiotic response elements (XRE), which are recognition motifs for xenobiotic compounds (7). Researchers have shown that AhR affects the Nrf2 pathway (a nuclear receptor that responds to electrophilic species) which will be discussed further later.

I. B. Cytochrome P450 2A6

Cytochrome P450 2A6 (CYP2A6) is one of three members of the CYP2A gene subfamily and is the most characterized of the three. CYP2A6 makes up only about 4% total hepatic CYP content, but is responsible for the metabolism of specific compounds such as nicotine, nitrosamines and aflatoxin B1, as well as several pharmaceuticals (5).

CYP2A6 is the only cytochrome P450 that is known to catalyze the coumarin 7-hydroxylation reaction at μM concentrations of substrate, making this compound an ideal probe substrate for this enzyme (5). **Figure I. 1** shows the reaction catalyzed by CYP2A6, which represents the conversion of coumarin into 7-hydroxycoumarin (11).

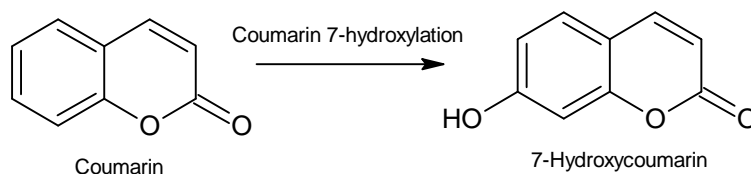


Figure I. 1: Coumarin 7-hydroxylation is catalyzed by CYP2A6.

I. B. i. CYP2A6-Active Site

The size of the active site of CYP2A6 is 25% of the other drug metabolizing CYPs, 2C8, 2C9, and 3A4. Due to tighter packing interactions, the active site is smaller, and more compact. Its' closed active site cavity is complementary to the size, shape and hydrophobicity of coumarin, and therefore favors substrates with more planar conformations (9). The carbonyl oxygen of coumarin is oriented to accept a hydrogen bond from Asn297. The Asn297 is the only polar residue that is accessible to the substrate indicating that a mostly hydrophobic substrate is preferred. Another interaction between the substrate and the binding pocket arises from the presence of Phe107, giving π stacking interactions. **Figure I. 2** shows these interactions providing for the proper orientation of the substrate, coumarin, so that the 7' carbon can be oxidized (10).

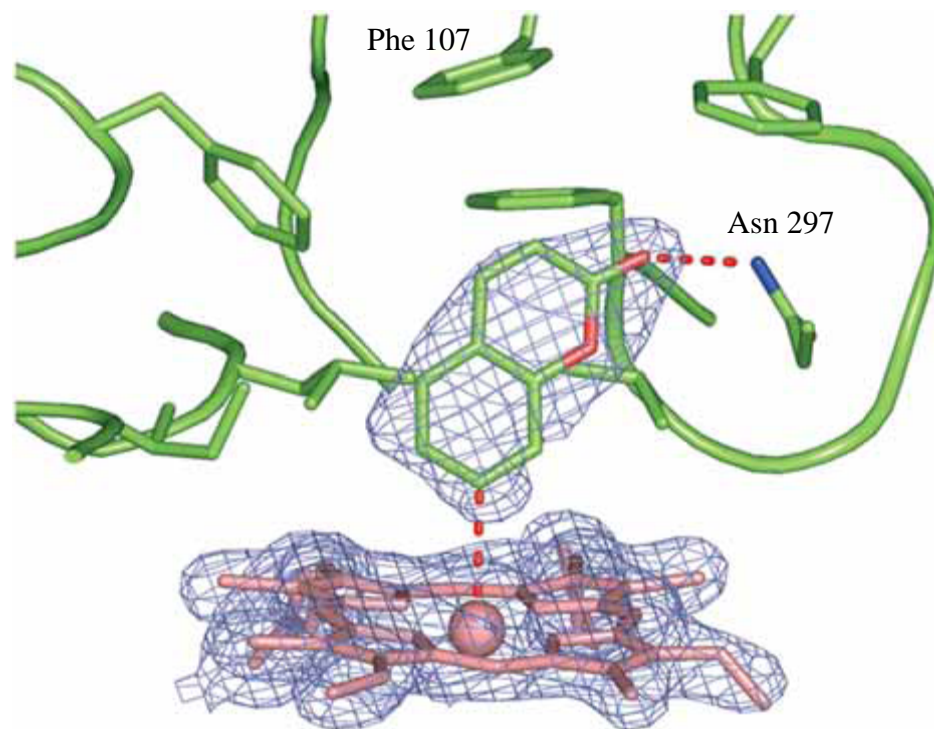


Figure I. 2: Structure of CYP2A6 with coumarin bound to the active site showing Phe 107 π stacking interactions, and Asn 297 H-bonding to the oxygen on the substrate (10).

I. B. ii. CYP2A6-Role in Nicotine Metabolism

According to several studies, CYP2A6 is the major P450 associated with nicotine metabolism. When nicotine enters the body, CYP2A6 oxidizes about 70% - 80% of the nicotine inhaled, by C-oxidation into cotinine (12). Cotinine is then further hydroxylated by CYP2A6, or is excreted from the body. Nicotine metabolism is very complex; it is not only oxidized into cotinine, but forms many other different products that have to go through further changes before excreted from the body. **Figure I. 3** depicts the mechanism by which nicotine gets oxidized by CYP2A6 into cotinine.

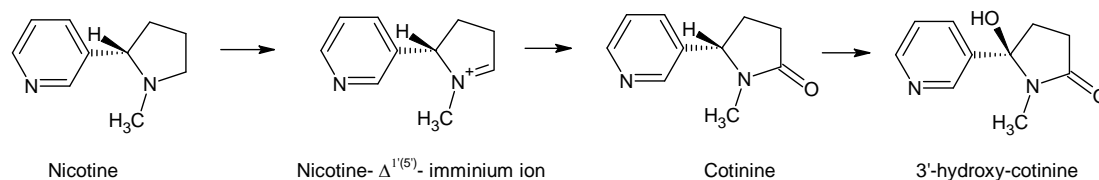


Figure I. 3: Metabolism Pathway of Nicotine into Cotinine. CYP2A6 catalyzes the conversion of nicotine into the iminium ion and also the hydroxylation of cotinine into 3'-hydroxy-cotinine. Aldehyde Oxidase converts the iminium ion into Cotinine.

I. B. iii. Smoking and CYP2A6 Role on Cancer Risk

It has been shown that inactivation of the CYP2A6 enzyme can alter nicotine inactivation rates and has the potential to alter smoking patterns (12). CYP2A6 is not generally associated with any adverse effects of drug metabolism. This suggests that inhibition of CYP2A6 would not alter drug metabolism. Researchers have found that a common inhibitor of CYP2A6, methoxsalen, decreases nicotine metabolism and smoking, suggesting that an inhibitor may be useful for smoking cessation (10). These studies underscore the need for further research on the CYP2A6, and in particular, identification of inhibitors of the enzyme.

Kamataki et. al. (25) have shown that CYP2A6 is responsible for all of the mutagenic activation of the tobacco related N-nitrosamines. They found a CYP2A6 polymorphism in Japanese that contained a deletion CYP 2A6*4C. They found that people that contained this deletion were unable to activate these tobacco related N-nitrosamines, thus showing a lower susceptibility to lung cancer that was induced by tobacco smoke. The researchers found that the frequency of the CYP2A6 deletions were lower in lung cancer patients when compared with healthy individuals. This suggested

that these healthy individuals had a resistance to carcinogenesis from N-nitrosamines because of the poor metabolism of them. They deduced from these findings that CYP2A6 is responsible for enhancing the risk for lung cancer. (25)

I. C. 2A6 Potential Inhibitors

The current study will focus on specific essential oils and aldehydes that have the ability to inhibit CYP2A6. Essential oils are the volatile lipid (oil) soluble part of different plants (4). These oils can be taken out of the plant matter by steam distillation. A variety of different aldehydes are present in each of the different oils that have been selected for this study. Cassia and cinnamon bark oil contain the aldehyde cinnamaldehyde, in fact based on GC/MS analysis of our Cassia oil, it was found that 80% of the total ion composition was cinnamaldehyde, which has the highest content of the essential oils looked at. Essential oil of Lemongrass on the other hand contains nearly 55% citral (4). The ability of these oils and their constituents to inhibit P450 2A6 may be of significance with regard to the role of 2A6 in nicotine or nitrosamine metabolism as noted previously.

The interest in aldehydes as inhibitors of P450 2A6 stems from prior studies by Raner et. al. indicating that aldehydes represent a general class of cytochrome P450 inhibitors (13). In particular, unsaturated aldehydes showed the greatest potency in the inactivation of several mammalian cytochrome P450s. The use of a series of related unbranched saturated and unsaturated aldehydes in the current study provides a means of probing structure/function relationships regarding inhibition of the smaller binding pocket of CYP 2A6 (10). CYP 2A6 has a few key amino acid residues that have been

shown above to play an important role in the binding specificity of inhibitors. These key amino acids are Phe 107 which provides for the π stacking interactions that would account for the preference of the unsaturated aldehydes or trans-cinnamaldehyde over saturated aldehydes (**Figure I. 2**). Also, Ans 297 has a H-bond to donate to a substrate and gives a higher preference for an inhibitor with a H-bond acceptor.

I. D. Phase II Enzymes- Anti-Oxidant Response

Vertebrates have developed a response network to cellular stresses that control reactive electrophiles by stabilization and activation of Nrf2, a transcriptional activator for a wide variety of antioxidant genes. Free radicals can be generated from exogenous and endogenous sources. Exogenous radicals occur from environmental oxidants such as O₃ and NO₂, ionizing radiation and bioactivated xenobiotics and drugs (18). Endogenous radicals can be generated within the cell from a one-electron transfer, to oxygen via monooxygenase enzymes such as cytochrome P450s. They can also be generated in the mitochondria via the production of ATP. Oxidative phagocytosis also result in free radicals generated in the lysosomes, and in the cell membrane free radicals result from the synthesis of inflammatory mediators (15).

The Phase II enzymes can be induced by a multitude of chemical species, including many of those found in the foods that we eat (16). Past research has shown that green tea polyphenolic compounds are good inducers of several Phase II enzymes in the body (20). There are two different types of inducers of Phase II enzymes, bifunctional and monofunctional. Bifunctional inducers act to induce Phase I and Phase II enzymes. Consequently, a bifunctional inducer results in an upregulation of Phase I enzymes

increasing the production of strong electrophiles, thereby promoting carcinogenesis, but also contributing to the production of Phase II enzymes. Monofunctional inducers only induce Phase II enzymes and consist of Michael addition acceptors, quinones and isothiocyanates. (18) The biochemical mechanism by which Phase II genes are induced is becoming clear. Under basal conditions, Nrf2 acts by complexing with Keap1 in the cytosol, and this complex is regulated via ubiquitination by CUL3 (18). Electrophiles modify the Keap1 and Nrf2 which allows Nrf2 to enter the nucleus and bind to promoter regions of target genes that contain antioxidant response elements and electrophilic response elements (ARE/EpRE), resulting in the induction (**Figure I. 4**) of over two hundred target genes (17).

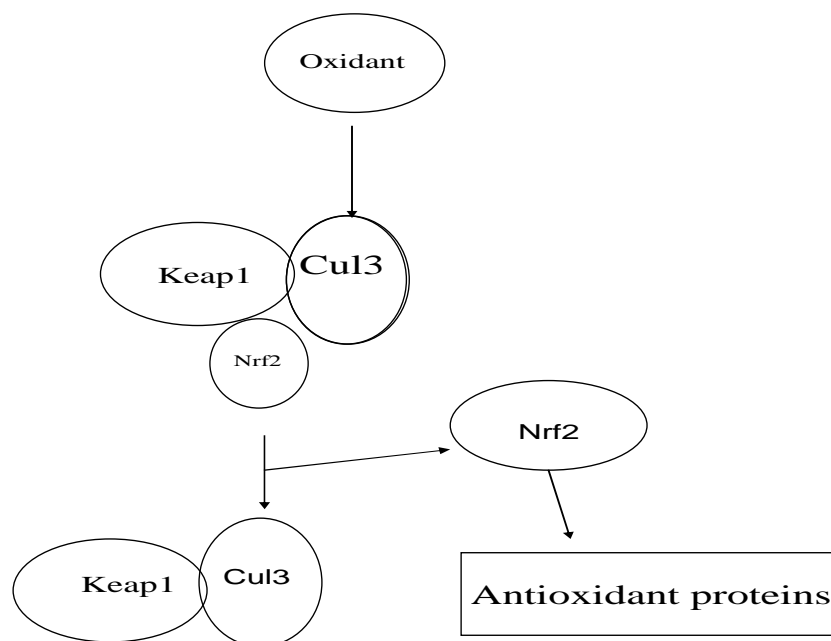


Figure I. 4: General overview of the mechanism in which the electrophile (oxidant) initiates the Nrf2 system. Once Nrf2 is activated and released from Keap1 it can move freely into the nucleus and turn on the ARE (18).

AREs act to regulate a multitude of antioxidant genes which respond to oxidative stressors such as reactive oxygen species. EpREs defend against electrophilic toxicity by controlling production of Phase II enzymes that detoxify electrophilic reactive metabolites (19). ARE/EpRE regulate the genes that code for antioxidant proteins, such as glutathione-S-transferase (GST), NAD(P)H: quinone oxidoreductase (NQO), and epoxide hydrolases (EPHX) (20). EPHX is responsible for metabolism of reactive epoxides, such as those found in cigarette smoke.

Genes that are responsive to this regulatory pathway include those involved in Phase II xenobiotic detoxification, antioxidant response, apoptosis, cell growth, and proteasomal activity (18). Common inducers of the system are H₂O₂, superoxide, hydroxyl radicals, quinones, and other electrophiles generated via lipid peroxidation (19). These electrophiles trigger a response by the Nrf2 system in which antioxidant response elements are turned on. The aldehyde groups present in the selected oils are of great interest due to their similarities to known electrophile inducers that are responsible for the induction of these Phase II enzymes. Recent studies have shown that electrophilic groups, such as aldehydes, may play a role in Nrf2-dependent induction of antioxidant genes in rats (11). For example, *N*-iodoacetyl-*N*-biotinylhexylenediamine (IAB) and polyphenols have been shown to be activators of the Nrf2 pathway (18). The hypothesis on which the current study is based is that the aldehyde constituents of the essential oils will play a role in the induction of antioxidant genes in HepG2 cells, causing a net antioxidant effect *in vivo*.

Prior studies aimed at understanding the Nrf2 pathway have focused on one of several different genes that are known to respond to oxidative stress. For example, Heme Oxygenase is a well known Phase II antioxidant protein that has two subtypes (22). Heme Oxygenase-1 (HO-1) catalyzes the breakdown of heme into two products, biliverdin and CO. Biliverdin reductase then converts biliverdin to bilirubin, which is a known protein antioxidant. (22) HO-1 is the rate limiting factor within the heme degradation. HO-1 is an inducible enzyme whereas HO-2 is a constitutive enzyme, not responding to oxidative

stressors. An increase in HO-1 mRNA levels is a response from oxidative stress caused by the depletion of reduced glutathione levels in the cell.

HO1 is also being used in the current study because of its known induction via a Nrf2-dependent pathway. Prior studies using green tea extracts have also pointed toward other potential antioxidant enzymes of interest which include histone-acetyl-transferase-1 (HAT1), Epoxide hydrolases (EPHX), and histamine N-methyl transferases (HNMT) (23). In the prior micro array experiments, all of these genes were induced in response to the presence of green tea extract, a suspected Nrf2 activator (20).

I. E. Balance of Phase I and Phase II Enzymes

The complex interplay between Phase I and Phase II enzymes can have a significant impact on the oxidative state of the cell, and can significantly impact the risk for developing diseases such as cancer (24). Phase I enzymes are involved in the oxidation of xenobiotics, and cytochrome P450s are the dominant enzymes in this class. In most cases, these xenobiotics are activated to form more hydrophilic species that can be removed more easily. Often, xenobiotics are activated to form electrophilic or free radical metabolites that can result in DNA adduct formation and oxidative stress. Phase II enzymes are required to relieve or prevent this oxidative stress, converting the activated metabolites to unreactive water soluble products to be excreted from the cell by Phase III enzymes (3).

CHAPTER II

MATERIALS AND METHODS

II. A. CYP 2A6 Inhibition Screening Method

The Michaelis-Menton model for enzyme inhibition has been used to look at the effects of the various essential oils on CYP2A6. The oils used included Cinnamon leaf, Lemon Grass, Coriander, and Cassia. In addition, a series of aldehydes were studied including α,β unsaturated aldehydes and saturated aldehydes ranging from four to twelve carbons. [E] Oct-2-enoic acid and Octenoic acid were also screened for inhibitory activity against CYP2A6. The assay that was used to measure inhibition of CYP2A6 was one that utilizes the conversion of coumarin into 7-hydroxycoumarin. The procedure was modified from that of Waxman and Chang, in which fluorometric analysis of the hydroxycoumarin was used [24]. Each inhibitor was initially diluted from 5 μL into 100 mL of water to make a stock solution. Conditions used for the screening experiment in the current study were as follows: Liver microsomes (1mg) were incubated in a reaction mixture containing 30 μM coumarin, potassium phosphate buffer containing 3.3mM MgCl_2 , (pH 7.4, 100 mM), serial dilutions of inhibitor (ranging from 5 μM to 600 μM for the purified aldehydes and 0.5 $\mu\text{g/mL}$ to 37.5 $\mu\text{g/mL}$ for the crude oils), and DI H_2O , added to give a volume of 450 μL . The reaction was initiated using 50 μL of a NADPH-regenerating system containing NADP^+ (1mM), glucose-6-phosphate (3.3 mM), and glucose-6-phosphate dehydrogenase (1 unit/mL), that was incubated for 7 minutes at

37°C prior to its' addition. Following a 30 minute incubation at 37 °C the protein was precipitated with 0.25 mL of 6% perchloric acid and placed on ice for 10 minutes.

Samples were centrifuged at 3500 rpm for 10 minutes, and 500 µL of the cleared solution and a 7-hydroxycoumarin standard were placed in HPLC vials to be analyzed via HPLC.

II. A. i. HPLC Analysis

HPLC analysis was performed using Shimadzu's LC-20AT/ Prominence Liquid Chromatography system and the samples were detected by the SPC-20A/ Prominence UV/Vis Detector at 320 nm. Up to 100 HPLC vials were loaded into the Autosampler and 40 µL of each sample were injected onto a RP-C18 HPLC column with a mobile phase consisting of 45% solution A (94% DI water, 5% methanol, and 1% acetic acid) and 55% methanol, at a flow rate of 1mL/min. Standards were used to differentiate the peaks of coumarin, and 7-hydroxycoumarin. The coumarin retention time of 6 minutes was determined by loading a coumarin standard. The retention time for the product, 7-hydroxycoumarin was determined using an authentic standard compound injected under the same conditions. This standard gave a retention time of 4.5 minutes. The 7-hydroxycoumarin peaks from each of the reaction samples were integrated to give the relative activities of the 2A6 in human liver samples.

II. A. ii. K_I Determination

Conditions used for determining the K_I in the current study were as follows: Liver microsomes (1mg) were incubated in a reaction mixture containing a range from 1 µM to 20 µM coumarin, potassium phosphate buffer containing 3.3mM MgCl₂, (pH 7.4, 100 mM), volume of inhibitor where in the screening conditions ~50% inhibition of 2A6, and

DI H₂O, added to give a volume of 450 μ L. The reaction was initiated using 50 μ L of a NADPH-regenerating system containing NADP⁺ (1mM), glucose-6-phosphate (3.3 mM), and glucose-6-phosphate dehydrogenase (1 unit/mL), that was incubated for 7 minutes at 37°C prior to its' addition. Following a 30 minute incubation at 37 °C the protein was precipitated with 0.25 mL of 6% perchloric acid and placed on ice for 10 minutes. Samples were centrifuged at 3500 rpm for 10 minutes, and 500 μ L of the cleared solution and a 7-hydroxycoumarin standard were placed in HPLC vials to be analyzed via HPLC.

Michealis Menton plots were used in order to determine the K_I for each aldehyde of interest. Each K_I was found by plotting V vs. [S] at a range of increasing concentration of coumarin in the presence and absence of an inhibitor. The inhibitor concentration was chosen based on screening experiments carried out to test the relative potency of each. Concentration of inhibitor, [I], was chosen where in the screening conditions ~50% inhibition of 2A6 was observed. The relative activity was plotted vs. concentration of coumarin using Slide Write Plus (by Advanced Graphics Software, Inc.). The Michealis Menton equation (**Equation II.1**) was used to determine the maximum velocity without inhibitor present (V_{max}), and with inhibitor present (V_{max app}), the substrate concentration at which in the enzyme is ½ the V_{max} (K_m), and the substrate concentration in the presence of inhibitor when the enzymes is at ½ the V_{max app} (K_{m app}).

$$V_o = \frac{V_{max} * [S]}{K_m + [S]} \quad \text{Equation II.1.}$$

Using Equation **II.2**, the K_I was calculated using the inhibitor concentration.

$$K_{m app} = K_m (1 + [I]/K_I) \quad \text{Equation II.2.}$$

The data supports the assumption that the inhibitors show the competitive model of inhibition, and V_{\max} was relatively unchanged by the presence of the inhibitor, for most of the compounds, indicating a competitive mode of inhibition.

II. B. HepG2- Cell Culturing

All procedures were carried out in a class II Laminar flow hood in a clean room. Human hepatoma cells (HepG2) were obtained from ATCC Laboratories cryopreserved in liquid nitrogen. The cells were rapidly thawed immediately before use. The cells were seeded onto an adherent T75 flask with Dulbecco's Modified Essential Medium with 4500 mg glucose/L to which 10% Fetal Bovine Serum was added. The cells were grown at 37°C until they reached 80% confluence (about 4 days). To split the cells the media was removed by aspiration and the cells were immediately washed with 3 mL of phosphate buffered saline (PBS) without $\text{Ca}^{2+}/\text{Mg}^{2+}$. This was to remove any residual trypsin inhibitor that may have been present. The PBS was then removed by aspiration and 3 mL Trypsin/EDTA (0.05% Trypsin) was added to each flask and the cells were bathed in this solution for 5 minutes. Cells were then loosened from the flask by tapping with the heel of the hand. For every 1 mL of Trypsin/EDTA added, at least 1 mL of media was needed to stop the trypsin reaction (3 mL media for a T75, 1 mL media for a T25). The cell suspension was then drawn into a glass pipette several times to mix thoroughly and 1 mL aliquots of the suspension were taken out and placed in T25's along with 4 mL of media to bring up to a final volume of 5 mL. The T25 flasks were grown out and further split into new cultures such that there were sets of four T25 flasks for use

in the induction of the phase II enzymes which will be discussed further in the next section.

For every passage of the cells, a single T75 flask was used to generate a stock culture for cryopreservation. This was done by taking either a T75 culture flask or seeding a new T75 flask from a T25 and aspirating the culture media once the cells reached 80% confluence. The cells were then washed with 3 mL of PBS. The cells were then trypsinized for 5 minutes and neutralized by adding an equal volume of DMEM. The flasks were tapped to remove cells from the surface, at which point they became suspended in the media. The cell suspension was drawn into a glass pipette and transferred to a 50 mL Falcon tube. The cells were spun down at 1000 rpm for 5 minutes into a pellet at room temperature and the supernatant was aspirated off. The cells were resuspended in 5 mL DMEM containing 10% DMSO and the cells were split into 1 mL aliquots and were transferred to cryovials, rapidly transferred to a freezer container and placed at -70°C for 4-5 hrs. The cells were then placed into the liquid nitrogen dewar for long term storage.

II. C. HepG2- Phase II Enzyme Induction

In order to show the induction of antioxidant genes by essential oil, four samples of HepG2 cells were grown in 5 mL of DMEM in T25 flasks until the cells reached 80% confluence. **Figure II. 1** shows the experimental setup of the incubations that were performed for the dose dependent experiments with cassia and trans-cinnamaldehyde. Cells were treated with various amounts of cassia oil and cinnamaldehyde and control cells were treated with equal quantities of sterile water. For the control, 4 mL of DMEM

and 1 mL of sterile water was added. Dose 1 through 3 contained 4 mL of DMEM and 1 mL of an oil/aldehyde mixture: 10 $\mu\text{g}/\text{mL}$, 20 $\mu\text{g}/\text{mL}$, and 100 $\mu\text{g}/\text{mL}$, respectively. Following treatment with inducer, cells were grown for an additional 5 hours at 37°C. For the time dependent study the control cells were immediately harvested without any further incubations at 0 minutes. For the others, they contained 1 mL of 20 $\mu\text{g}/\text{mL}$ inducers (cassia and cinnamaldehyde) and 4 mL of DMEM and were incubated at 37°C time intervals of 1, 6, and 24 hours.

Figure II. 2 shows the experimental setup of the incubations that were performed for the time dependent experiments with cassia and trans-cinnamaldehyde. The cells were treated with 1 mL of 20 $\mu\text{g}/\text{mL}$ cassia and cinnamaldehyde and 4 mL of DMEM. The control cells were immediately harvested and the RNA was isolated. Time 1 through 3 were incubated at 37°C for 1 hour, 5 hours, and 24 hours, respectively.

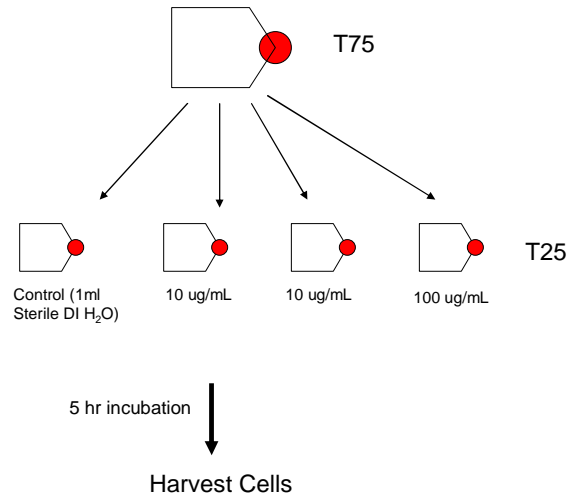


Figure II.1: Experimental setup for dose dependent studies probing for the induction of Phase II enzymes in HepG2 cells. T75 culture flask were split at 80% confluence into four experimental T25 culture flasks. Concentrations of 10 $\mu\text{g}/\text{mL}$, 20 $\mu\text{g}/\text{mL}$ and 100 $\mu\text{g}/\text{mL}$ of cassia oil and trans-cinnamaldehyde administered to the T25 as mentioned above. After a 5hr incubation the cells were harvested for RNA isolation.

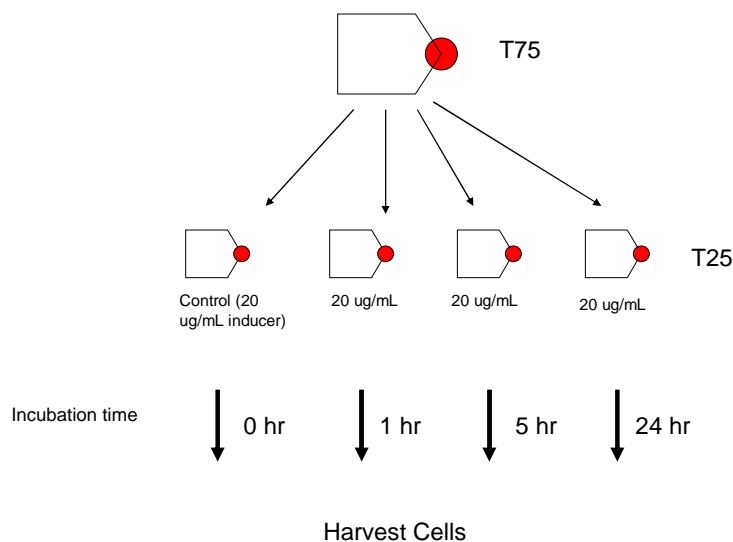


Figure II.2: Experimental setup for time dependent studies probing for the induction of Phase II enzymes in HepG2 cells. T75 culture flask were split at 80% confluence into four experimental T25 culture flasks. A concentration of 20 $\mu\text{g}/\text{mL}$ of cassia oil and trans-cinnamaldehyde was administered to the T25 as mentioned above. After a 0, 1, 5, and 24 hour incubation the cells were harvested for RNA isolation.

II. D. Total RNA Isolation and Purification

Prior to RNA isolation, the solutions were prepared by adding 200 μL Beta-mercaptoethanol to 10 mL of the SV RNA Lysis Buffer, 275 μL of nuclease free water to the DNase I, 100 mL of 95% ethanol to the SV RNA Wash Solution and 8 mL 95% ethanol to the SV DNase stop solution. The cells were harvested and the total RNA was isolated using the SV total RNA isolation system by Promega. Cultured Cells were harvested by first aspirating off the DMEM and washing with 1 mL PBS. The 1mL of RNA lysis buffer was added to each flask to which the cells were adhered. After bathing the cells for 1 minute in the buffer, a cell scrapper was used to physically remove the

cells from the flask, where they became suspended in the lysis buffer. Following lysis, 175 μ L of the lysed sample was mixed with 350 μ L of the RNA dilution buffer in a 1.5 mL eppendorf tube and were inverted several times to fully dilute the RNA. Samples were then incubated at 70°C for three minutes (longer than three minute incubation may compromise the RNA). Samples were centrifuged for 10 minutes at 14,000 x g at room temperature to pellet the remainder of the unwanted cell debris leaving RNA in the Dilution Buffer.

The total isolated RNA was purified by the centrifugation method as follows: the cleared lysate that contained the RNA was transferred to a new tube to be purified. A 200 μ L volume of 95% ethanol was added and the entire content of the tube was transferred to the spin column assembly and then centrifuged for one minute at 14,000 x g. After every centrifugation in the purification, the liquid in the collection tube was discarded. The RNA was then washed with 600 μ L of RNA wash solution. DNase incubation mix, containing 40 μ L yellow core buffer, 5 μ L 0.09M MnCl₂ and 5 μ L DNase1 enzyme was combined and then added to each reaction making sure that the entire membrane was covered. The DNase solution was incubated for 15 minutes at room temperature. To stop the reaction, 200 μ L of DNase stop solution was added to the spin basket and then centrifuged for one minute at 14,000 x g. Two RNA washes were then performed by adding 600 μ L and 250 μ L of RNA Wash Buffer followed by centrifugation for one minute and two minutes, respectively. The spin basket was then placed in an elution tube and by adding 100 μ L of Nuclease-Free water and centrifuging for one additional minute, the RNA was eluted. The purified RNA was then stored at -

70°C in microfuge tubes. The RNA was quantified by spectral absorption by adding 0.6 mL of DI water and 5 µL purified RNA and mix briefly into a cuvette. The absorption was read at 260 nm to give a crude amount of the RNA present in each sample. Using Beer's Law $A = e \cdot C \cdot l$, with an extinction coefficient of 25 µl/µg/cm the concentration of the RNA can be calculated.

II. E. RT-PCR of Purified RNA Samples

Following the RNA isolation, RT-PCR was performed to show the induction of the Phase II enzymes using 1.21 µg/µl of RNA. The genes that were probed include epoxide hydrolase (EPHX1), histone acetyltransferase1 (HAT1), histamine N-methyltransferase (HNMT), and Heme Oxygenase 1 (HO-1). The internal controls used were β-actin and GAPDH. **Table II. 1** shows the 5' -3' sequence of the upstream and downstream primers used for the amplification of these enzymes as well as the corresponding expected product sizes. All primers were synthesized and purchased from Integrated DNA technologies Inc. (IDT). The 25 µL reaction, consisted of a final concentration of 1x AMV/*Tfi* Reaction Buffer (Promega), 1mM MgSO₄, 0.2 mM dNTPs, 1 µM forward and reverse primers, 1.21 µg template DNA, *Tfi* DNA polymerase (0.1 u/µL), AMV Reverse Transcriptase (0.1u/µL) and Nuclease free water to reach the final volume. RNA was first converted into cDNA via the reverse transcriptase (RT) reaction, which was carried out at 45°C for 45 minutes. Following RT, the PCR reactions were run using the Gene Amp PCR System 9600 (Perkin Elmer Cetus), with an initial denaturation and deactivation of reverse transcriptase at 95°C for 2 minutes and were followed by PCR cycling for 30 cycles. The cycles consisted of a denaturing step at 95°C for 30 seconds,

followed by a 60 second annealing temperature that varied with the each different primer (shown in figure 1), and then an extension step of 2 minutes at 72°C. The sample was cooled to 4°C until it was removed from the thermal block for analysis. The samples were then either immediately analyzed by agarose gel electrophoresis or stored at -20°C for use at a later time.

Table II.1- List of primer sequences, product size and annealing temperature used to show Phase II enzymes induction.

Primer	Sequence	Product (bp)	Annealing temperature
β-actin	5' AGCGAGCATCCCCAAAGTT 3'; 5' GGGCACGAAGGCTCATCATT 3'	285	56
GAPDH	5' AGAAGGCTGGGGCTCATTTG 3'; 5' AGGGGCCATCCACAGTCTTC 3'	258	57.5
HAT1	5' CAGTTCTCAGTCCAACAGGAGGAG 3'; 5'CGGTCGCAAAGAGCGTAGCTCCA 3'	215	62
HNMT	5' GGACAAGAAGCTGCCAGGC 3'; 5' CTCGAGGTTTCGATGTCTTGCC 3'	219	60
EPHX1	5' GGCTTCTCAGAGGCATCCTCC 3'; 5' CCACATCCCTCTCAGTGAGGCC 3'	273	59
HO1	5' CAGGCAGAGAATGCTGAGTTC3' 5' GCTTCACATAGCGCTGCA 3'	270	55

II. F. Gel Agarose

The RT-PCR products were then visualized using gel electrophoresis. A 2% gel was made using 0.6 g of GCA Agarose (ISC Bio Express) and 35 mL 1X TRIS-Acetate EDTA solution (TAE) containing 40 mM TRIS-Acetate, and 1 mM EDTA. The solution was placed in a microwave a heated into totally liquefied and was poured into the gel box and was allowed to set for an hour. Then the gel was added to the BioRad Mini-Sub Cell

GT box such that the wells were closest to the black terminal and 1 X TAE buffer was added up to the fill line. Sample loading buffer (4 μ L) was added to each sample and then 10 μ L aliquots of the samples containing the amplified DNA were loaded into each well. A 5 μ L sample of a 100-1300bp ladder was also analyzed as a standard to show band sizes. The gels ran at 110 volts using the BioRad Power Pac 300 for approximately 45 minutes until the bromophenol blue tracking dye reached approximately $\frac{3}{4}$ of the way to the end of the gel. The gel was visualized by staining with 30 μ L of 0.625 mg/mL ethidium bromide for 30 minutes in 1 X TAE buffer and then destained using DI water for 15 minutes. The gel was then visualized under UV light and imaged using a Kodak digital imaging system.

CHAPTER III
RESULTS AND DISCUSSION

III. A. Inhibition of CYP2A6

The interaction of CYP2A6 with a diverse set of aldehydes leads to inhibition of the enzyme, which has been shown using an enzymatic assay for the 7-hydroxylation of coumarin with HPLC detection. This assay was developed in our lab for the purpose of high throughput HPLC analysis of P450 2A6 inhibitors. **Figure III. 1** shows a HPLC chromatogram of a 7-hydroxycoumarin standard. The reaction mix loaded contained all of the components in the assay except for coumarin. The peak that was seen at 2.5 was identified as NADPH by leaving out NADPH in the following reaction. The peak at 4.5 minutes was determined to be 7-hydroxycoumain. A peak with a retention time of around 4.5 minutes was observed in subsequent experiments in which the substrate coumarin was incubated with human liver microsomes and NADPH. In control experiments where NADPH was omitted, this peak was not observed, confirming its identity in the catalytic assays. Prior studies involving P450 2A6 utilized a fluorescent method of detection of the 7-hydroxycoumarin, however in this lab, fluorescence measurements were inconsistent probably due to the non-specific nature of the assay. The HPLC method was therefore developed to overcome these difficulties.

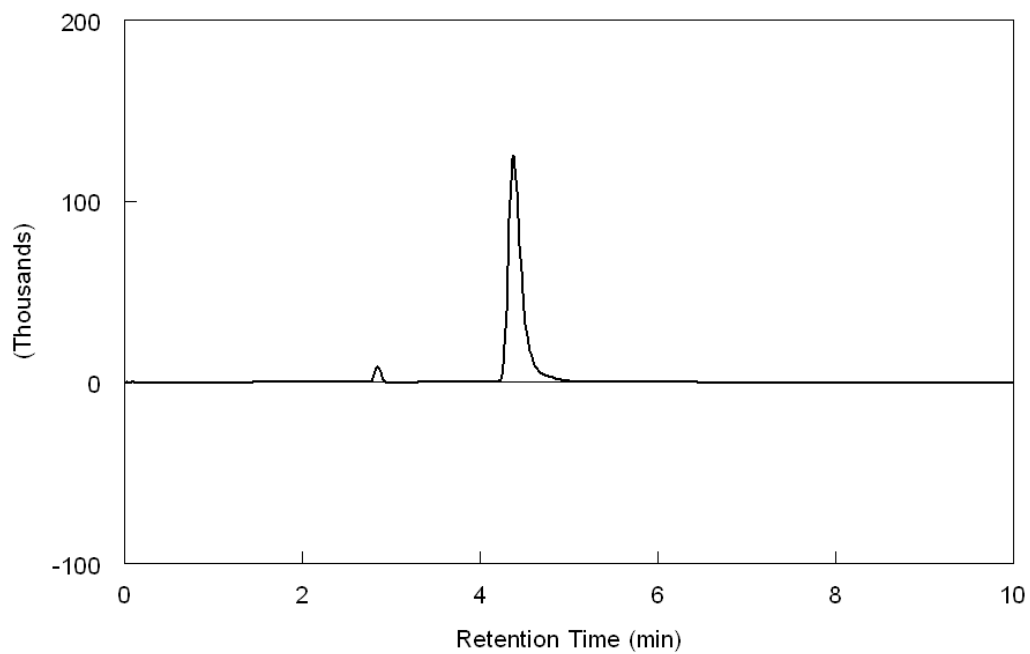


Figure III. 1: 7-Hydroxycoumarin standard HPLC chromatogram containing 7-hydroxycoumarin. The other reaction components are described in the experimental section, and lacks coumarin. The peak at 4.5 minutes was identified as the 7-hydroxycoumarin standard. The small peak at 2.3 min. was due to a small amount of NADPH.

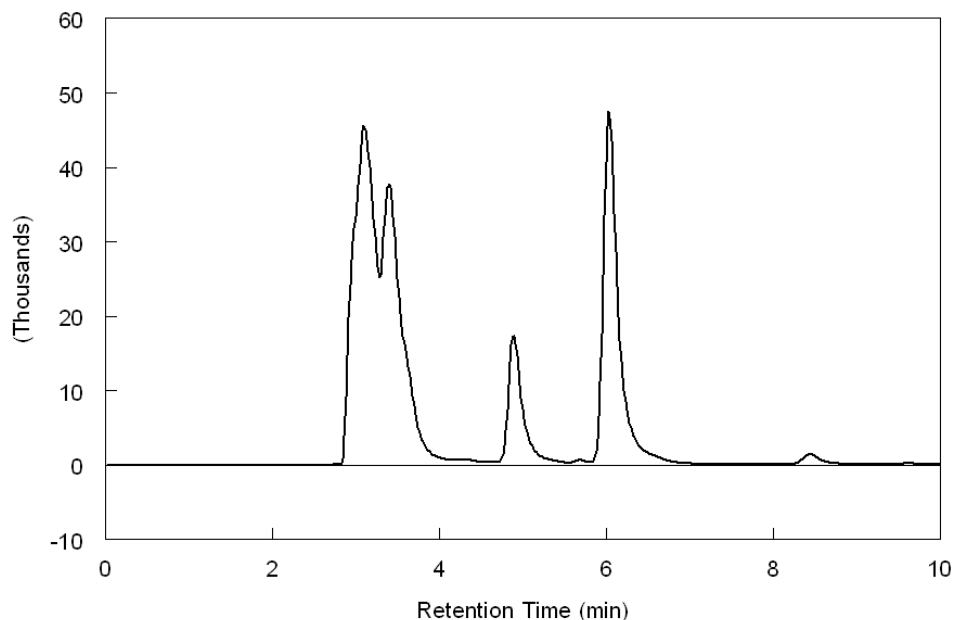


Figure III. 2: A sample of a HPLC chromatogram obtained with the 7-hydroxylation assay. The peak with a retention time of 6 minutes was identified as coumarin, at 4.5 minutes the peak of 7-hydroxycoumarin was seen, and at a retention time of 2.5 min. NADPH was seen. These retention times were determined by comparison with standards each of the compounds. This sample contained 20 μM coumarin, potassium phosphate buffer containing 3.3mM MgCl_2 , (pH 7.4, 100 mM), 0.0754 mM trans-2-octenal and 1mM NADPH and was incubated for 7 minutes at 37°C.

III. A. i. Essential Oils Inhibition Analysis

Initial screening experiments in this lab indicated that the essential oil of cassia significantly inhibited CYP2A6. The essential oils were included in the reaction of CYP2A6 with 30 μM coumarin with increasing the concentration of oil from 0.5 $\mu\text{g/mL}$ to 37.5 $\mu\text{g/mL}$. **Figure III. 3** shows the inhibition of P450 2A6 by the essential oils of cassia, cinnamon leaf, coriander, and lemongrass. As seen in this figure, of these four

oils, only cassia inhibited the activity of 2A6 by >50% at concentrations as low as 12.5 ug/mL. In fact, lemon grass, which was the next most potent oil showed only 50% inhibition where cassia oil inhibited 2A6 activity by 80% at the highest concentration. For this reason cassia oil was selected for subsequent studies with regard to its inhibition on P450 2A6. Since the main aldehyde in cassia oil is cinnamaldehyde, it is likely that this compound is responsible for inhibition. From this it can be estimated that the amount of inhibition for cinnamaldehyde should exceed that of the essential oil of cassia, assuming cinnamaldehyde is the only inhibitory compound present in the oil. The essential oil of lemongrass, which contains 55% citral, showed inhibition around 50% on CYP2A6 at the highest concentration. The cinnamon leaf oil showed little to no inhibition on CYP2A6. Cinnamon Leaf oil contains 70-90 % eugenol and only 5% cinnamaldehyde. Coriander shows roughly 20% inhibition of the activity of CYP2A6 (contains 20% hydrocarbons and 45-70% d-linalool, and coriandrol). All of these observations point to cinnamaldehyde as a relatively potent chemical inhibitor of P450 2A6.

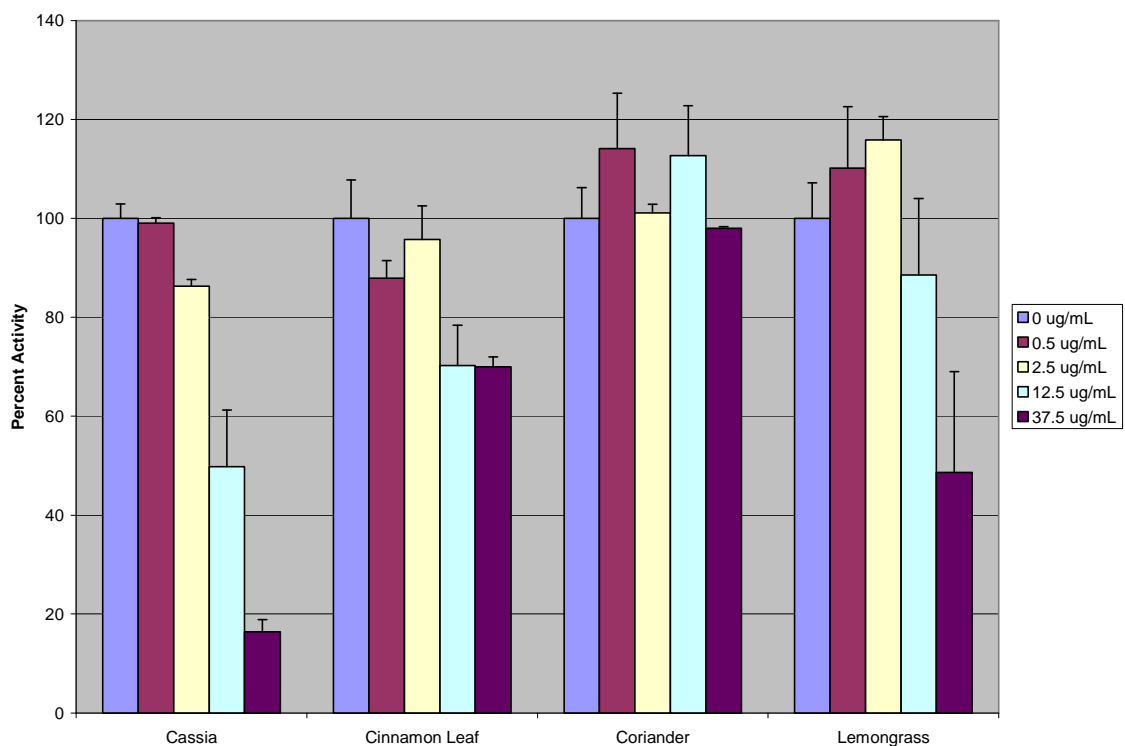


Figure III. 3: Plot of percent activity of CYP2A6 using human liver microsomes in the presence of 30 μ M coumarin, different essential oils from 0.5 μ g/mL to 37.5 μ g/mL and 1 mM NADPH.

III. A. ii. Individual Aldehyde Effects on CYP2A6

The effects of essential oils as inhibitors of CYP2A6 have been shown most effectively with cassia and lemon grass. The effect on CYP2A6 that the cinnamaldehyde may possess, based on the results shown for the essential oil of cassia, was further examined because of the fact that cinnamaldehyde composed of approximately 80% of the cassia oils. Also a variety of saturated and unsaturated aldehydes were used to probe for inhibition on CYP2A6 activity in order to better understand the structural features of the aldehydes that make them inhibitors of this particular cytochrome P450.

III. A. ii. a. Aromatic Aldehydes as CYP2A6 inhibitors

To probe the effect that aromatic aldehydes have on CYP2A6 the compounds cinnamaldehyde and benzaldehyde were used. CYP2A6 when in the presence of coumarin and increasing concentrations of cinnamaldehyde shows 89.4% inhibition at the highest concentration of inhibitor, as shown below in **Figure III. 4**. Even at 12.5 $\mu\text{g/mL}$, inhibition of 2A6 by cinnamaldehyde was nearly 60%, which is consistent with observed inhibition of 2A6 using cassia oil. Benzaldehyde was another aromatic aldehyde of interest because of its structural similarities to cinnamaldehyde. When in the presence of increasing amounts of benzaldehyde and constant concentrations of coumarin, CYP2A6 activity drops to 23.1% activity at the highest concentration of inhibitor. The screening results for benzaldehyde are shown in **Figure III. 4**. Concentrations are shown in screening data using $\mu\text{g/mL}$ but in Michaelis Menton plots concentrations are converted into mM units using the molecular weight of the aldehydes. Although not as potent as cinnamaldehyde in its inhibition of 2A6, benzaldehyde was still a moderately potent inhibitor.

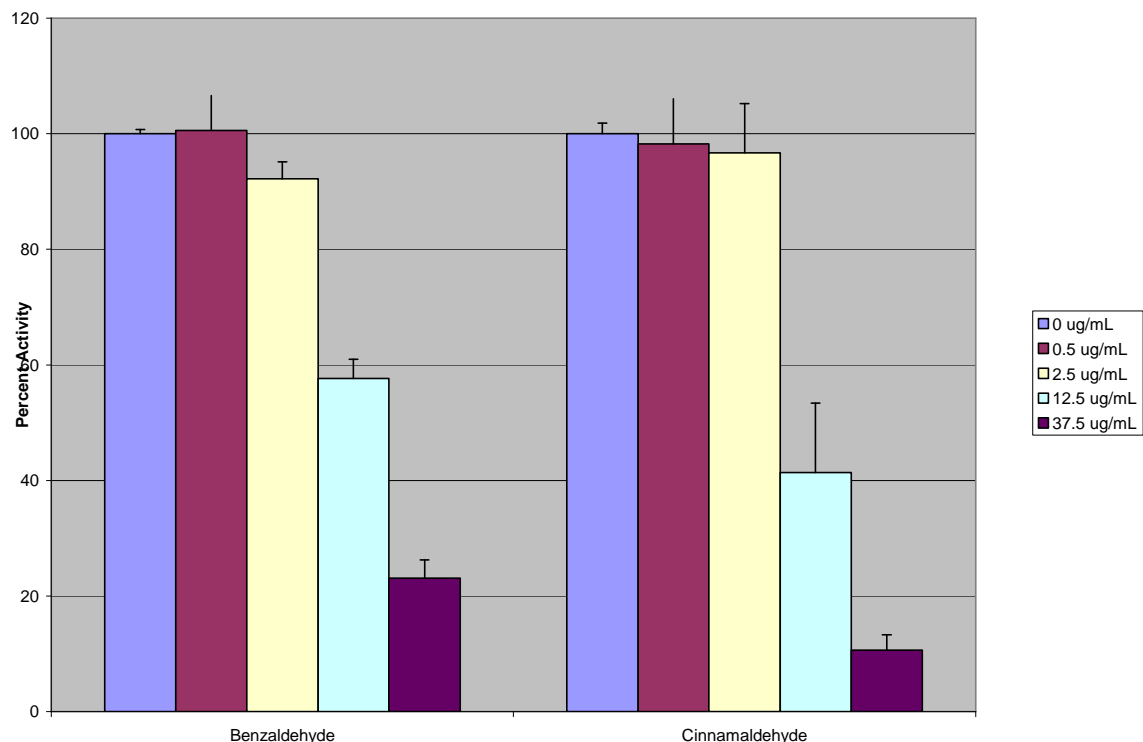


Figure III. 4: Screening of Aromatic Aldehydes, benzaldehyde and cinnamaldehyde. The reaction probing for the activity of CYP2A6 used a range from 0 $\mu\text{g/mL}$ to 37.5 $\mu\text{g/mL}$ aldehydes, 30 mM coumarin, human liver microsomes, and NADPH.

To probe further into the effects of the essential oil of cassia, cinnamaldehyde was examined using the Michaelis Menten model of enzyme kinetics and inhibition. CYP2A6 was incubated with cinnamaldehyde and coumarin using different concentrations of substrate ranging from 1 μM to 20 μM . The experiment was carried out in the presence and absence of cinnamaldehyde (0.0605 mM) and the relative activities were plotted against the concentration of coumarin as in the Michaelis Menton model. Based on the data shown in this plot (**Figure III. 5**), a V_{max} and K_{M} were calculated in the absence and presence of cinnamaldehyde. Based on the observation that V_{max} was unaffected, the competitive model of inhibition was used to calculate a K_{I} of 0.0214 mM for

cinnamaldehyde. Based on the obtained values for K_i of the cinnamaldehyde in this experiment, and its relative abundance in cassia oil, we can assume that cinnamaldehyde is primary inhibitor of CYP2A6 contained in the cassia oil.

The ability of benzaldehyde and trans-cinnamaldehyde to inhibit the enzyme is attributed to the presence of the unsaturated bonds in the compounds. These compounds both have a benzyl group within the molecule which mimics part of the substrate, coumarin. Even though coumarin has a bicyclic ring, trans-cinnamaldehyde closely resembles coumarin's size and shape, which could possibly result in its' ability to compete in the enzyme's active site.

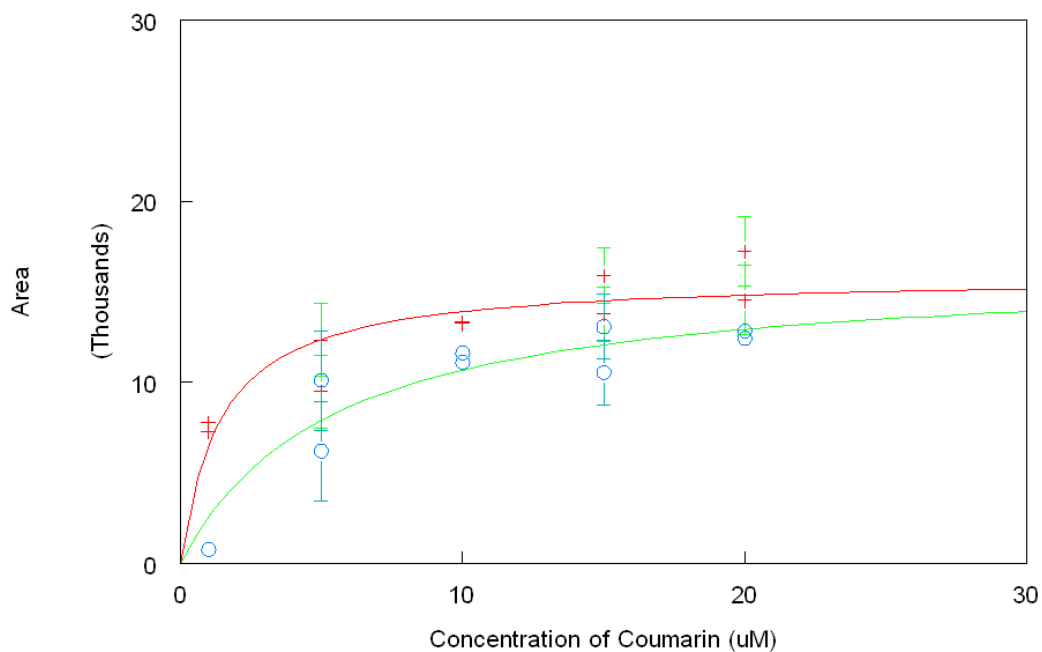


Figure III. 5: Plot of area vs. coumarin concentration in the presence (red) and absence (green) of trans-cinnamaldehyde (0.0605 mM). Reactions contained inhibitor, human liver microsomes, a range of substrate concentrations from 0 μ M to 20 μ M, and 1 mM NADPH.

III. A. ii. b Structure/Activity Relationship: Saturated vs. Unsaturated Aldehydes

To analyze the effect of bond saturation on the inhibition of CYP2A6, a series of saturated and unsaturated aldehydes were used. First, inhibition screening of a broad range of saturated and unsaturated aldehydes were performed using increasing amounts of aldehydes in the presence of CYP2A6 and coumarin. **Figure III. 6** shows a broad range screen of aldehydes containing saturated bonds, as well as a select set of essential oils, and acids. These aldehydes showed a relatively low amount of inhibition on CYP

2A6 activity. Undecylic aldehyde was the only saturated aldehyde to show any kind of inhibition to a 77% activity of the enzyme at the highest concentration 37.5 $\mu\text{g/mL}$ of aldehyde. All of the other compounds have little to no inhibition on CYP 2A6. **Figure III. 7** shows the percent inhibition of CYP 2A6 with increasing concentrations of unsaturated aldehydes. The most notable compounds are trans-2-hexenal, and trans-2-octenal. Trans-2-hexenal shows 59% activity of the enzymes at the mid-range concentration and at the high end concentration the enzymes is only 27% active. Trans-2-octenal shows at the highest concentration of aldehyde the activity dropped to merely 23%. The smallest compounds such as trans-2-pentenal and crotonaldehyde inhibited 2A6 at only 82% enzymes activity when in the presence of crotonaldehyde at the highest concentration, and 60.4% activity of the enzymes with trans-2-pentenal present at the highest concentration. Trans-2-nonenal shows inhibition to about 44% activity of the enzyme.

Based on these studies it appeared that the degree of saturation of the aldehyde influenced the potency of inhibition of the enzyme. Based on the active site of CYP 2A6 it might be predicted that the unsaturated aldehydes would be preferred, which is consistent with the screening data from **Figure III. 6** and **Figure III. 7**.

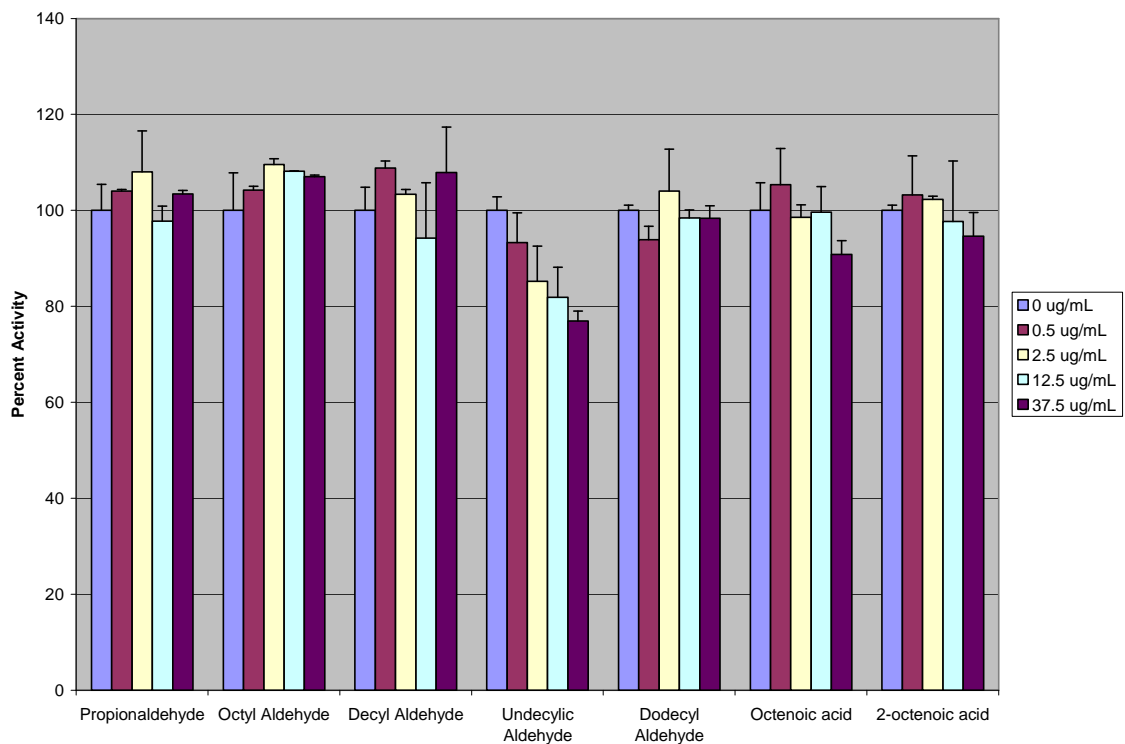


Figure III. 6: The reaction probing for the activity of CYP2A6 used a range of inhibitors (saturated aldehydes and carboxylic acids) from 0 $\mu\text{g}/\text{mL}$ to 37.5 $\mu\text{g}/\text{mL}$, 30 mM coumarin, human liver microsomes, and NADPH.

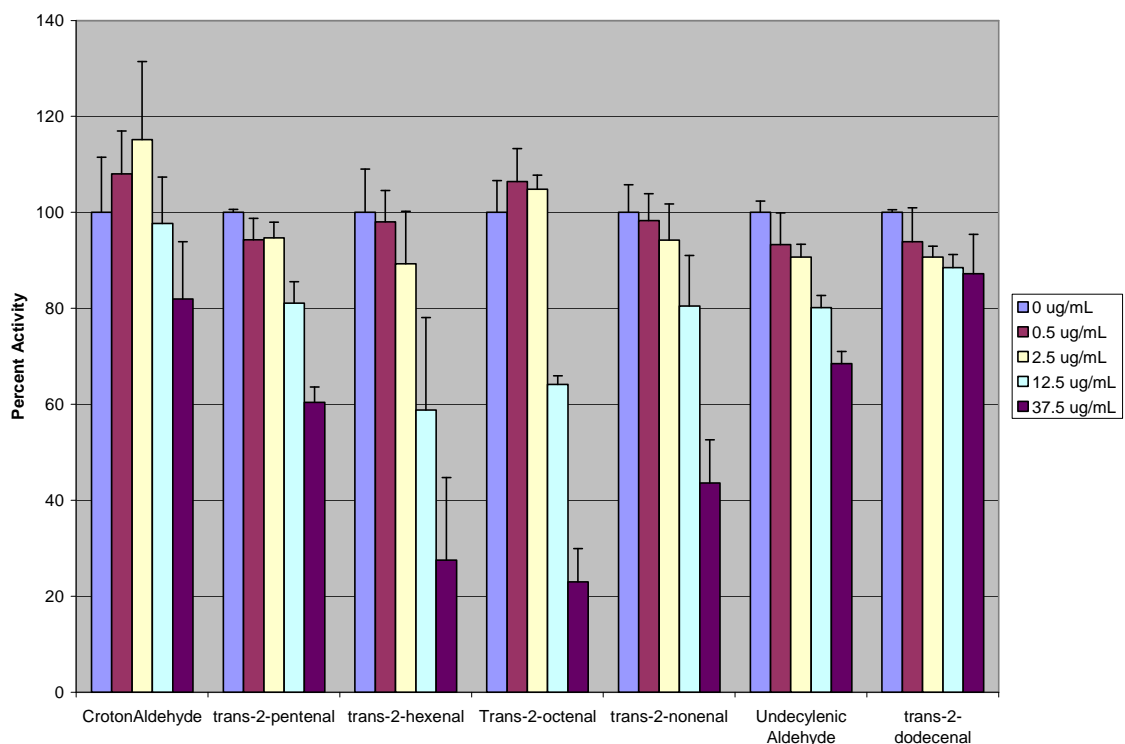


Figure III. 7: The reaction probing for the activity of CYP2A6 used a range of inhibitors (unsaturated aldehydes) from 0 $\mu\text{g/mL}$ to 37.5 $\mu\text{g/mL}$, 30 mM coumarin, human liver microsomes, and NADPH.

III. A. ii. c. Structure/Activity Relationship: Aldehyde Chain Length

Once the effects of saturated and unsaturated aldehydes were differentiated, and that it was determined that unsaturated aldehydes were more inhibitory than saturated aldehydes, the focus was turned to the effect of the chain length on CYP2A6. **Figure III. 7** shows the broad range screen of the unsaturated aldehydes with increasing concentration. As seen, the activity of CYP2A6 decreases the most around 6-8 carbon chain lengths. In order to determine the potency of these compounds, Michaelis-Menton plots were generated in the presence and absence of inhibitor and relative activities of 2A6 were plotted against the concentration of the substrate coumarin (1 μM to 20 μM). A

Michaelis-Menton plot was created for each of the following aldehydes: crotonaldehyde, trans-2-pentenal, trans-2-hexenal, trans-2-octenal, trans-2-nonenal, and trans-cinnamaldehyde. Each individual aldehyde was used at the approximate concentration that led to 50% inhibition on CYP2A6 in the screening reactions and was analyzed by plotting the integrated product peak area vs. substrate concentration. **Figures III. 8 - III. 12** are Michaelis-Menton plots that show the formation of 7-hydroxycoumarin with and without aldehyde with increasing concentrations of coumarin. In some cases the mode of inhibition appeared to be competitive based on a constant V_{\max} with and without inhibitor and the others showed a slight difference in the V_{\max} and a percent error reasonable to make the assumption that they are competitive inhibitors, along with an increase in the K_M with the presence of the inhibitor. The Michaelis-Menton plot using 0.557 mM crotonaldehyde is shown in **Figure III. 8**. Crotonaldehyde's calculated value for K_I was 0.205 mM showing a moderate potency compared to the other aldehydes. **Figure III. 9** shows the Michaelis-Menton plot was 0.464 mM trans-2-pentenal. Trans-2-pentenal had a K_I of 0.172 mM. The Michaelis-Menton plot shown in **Figure III. 10** is of 0.133 mM trans-2-hexenal, giving a K_I of 0.0196 mM. The Michaelis-Menton plot of trans-2-octenal at a concentration of 0.075 mM is depicted in **Figure III. 11**. with a K_I of 0.0278 mM. **Figure III.12** shows the Michaelis-Menton plot for 0.186 mM trans-2-nonenal with a K_I of 0.0327 mM.

Table III. 1 shows the V_{\max} and $V_{\max \text{ app}}$ for the aldehydes being used. The calculated values for K_M , $K_{M \text{ app}}$, and K_I are listed in **Table III. 2** for each aldehyde. These values were calculated according to **Equations II.1** and **II.2**. The rate at which

CYP2A6 is at $\frac{1}{2}$ its maximum velocity, K_M , were consistent at a concentration of substrate around the 2 to 3 μM range (**Table III. 2**).

Based on the chain length, the more potent inhibitors were trans-2-hexenal, trans-2-octenal, which gave K_I values near 0.02 mM. These results are fully consistent with those obtained in the initial screening experiments. The V_{max} and $V_{\text{max app}}$ reached approximately the same value, leading to the assumption that all of the unsaturated aldehydes listed are competitive inhibitors.

As the straight chain unsaturated aldehydes deviate away from a 6-8 carbon chain length, the inhibition dramatically decreases. The ability of these compounds to inhibit CYP2A6 shows that the hypothesis was correct about the need for an α,β unsaturated bond, as well as the need for a smaller compound with about seven or eight carbons long. Again the experimental data support an active site structure that is highly constrained and binds to substrates via π -stacking interactions.

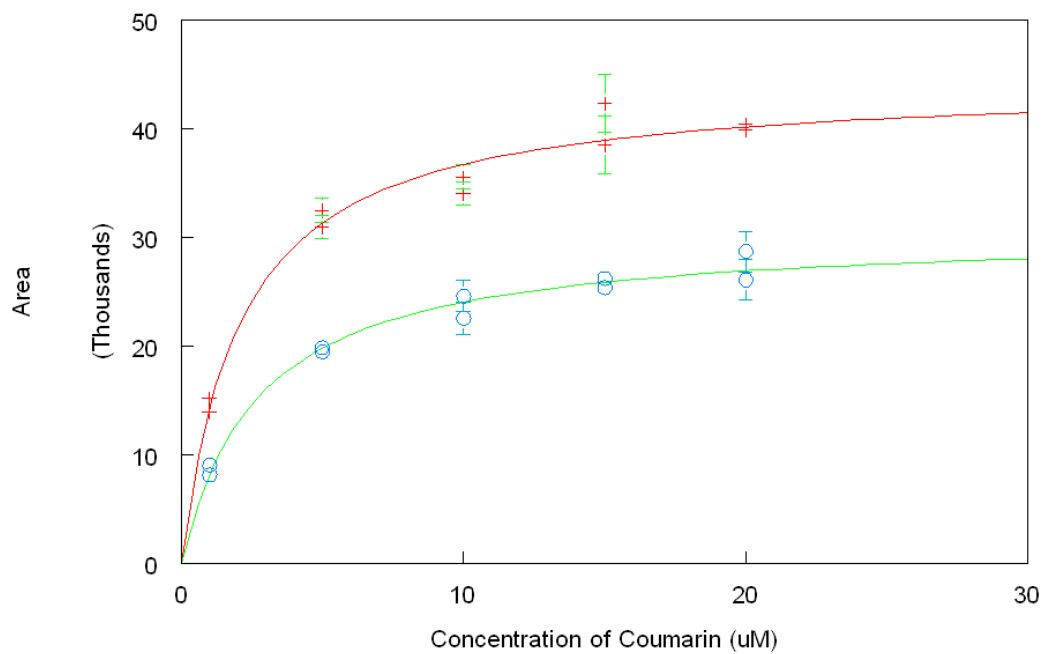


Figure III. 8: Plot of area vs. coumarin concentration in the presence (red) and absence (green) of crotonaldehyde (0.557 mM). Reactions contained inhibitor, human liver microsomes, a range of substrate concentrations from 0 μM to 20 μM , and 1 mM NADPH.

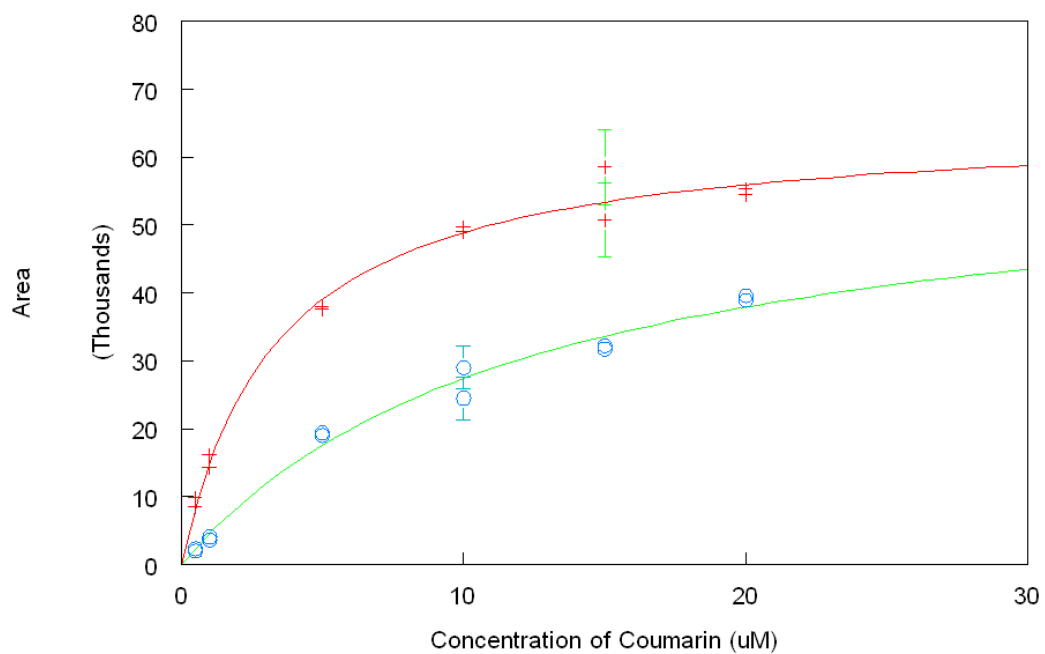


Figure III. 9: Plot of area vs. coumarin concentration in the presence (red) and absence (green) of trans-2-pentenal (0.464 mM). Reactions contained inhibitor, human liver microsomes, a range of substrate concentrations from 0 μ M to 20 μ M, and 1 mM NADPH.

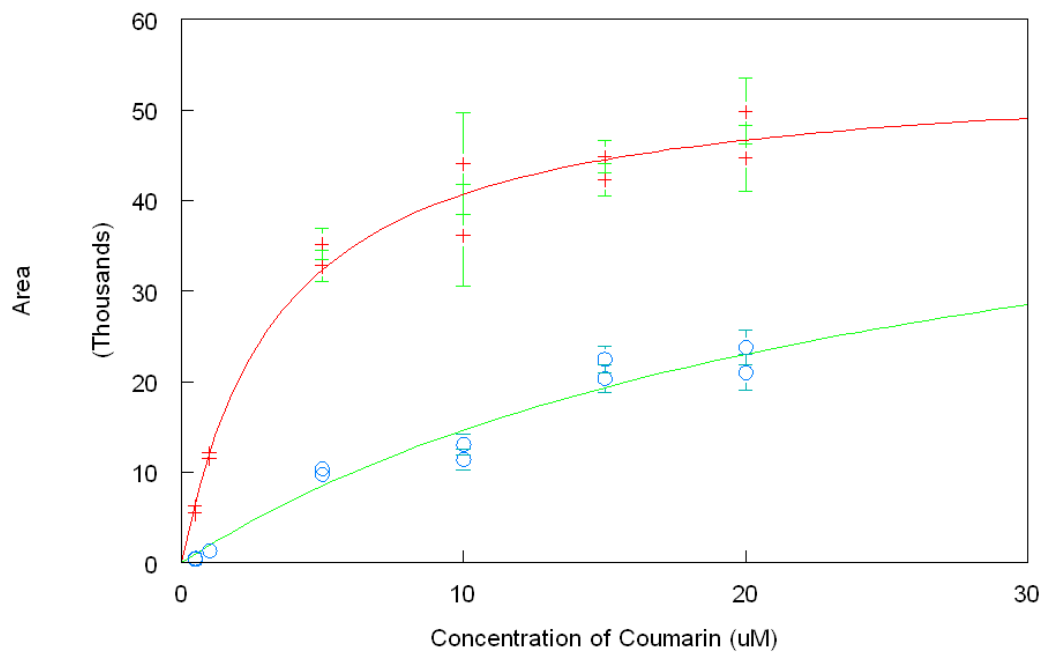


Figure III. 10: Plot of area vs. coumarin concentration in the presence (red) and absence (green) of trans-2-hexenal (0.133 mM). Reactions contained inhibitor, human liver microsomes, a range of substrate concentrations from 0 μM to 20 μM , and 1 mM NADPH.

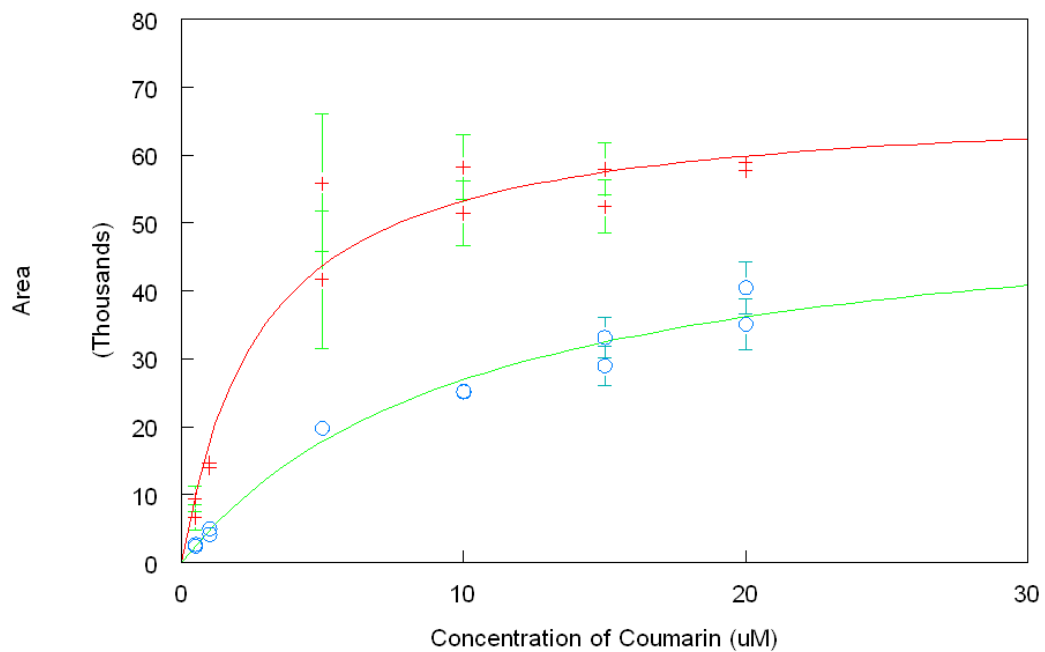


Figure III. 11: Plot of area vs. coumarin concentration in the presence (red) and absence (green) of trans-2-octenal (0.0754 mM). Reactions contained inhibitor, human liver microsomes, a range of substrate concentrations from 0 μ M to 20 μ M, and 1 mM NADPH.

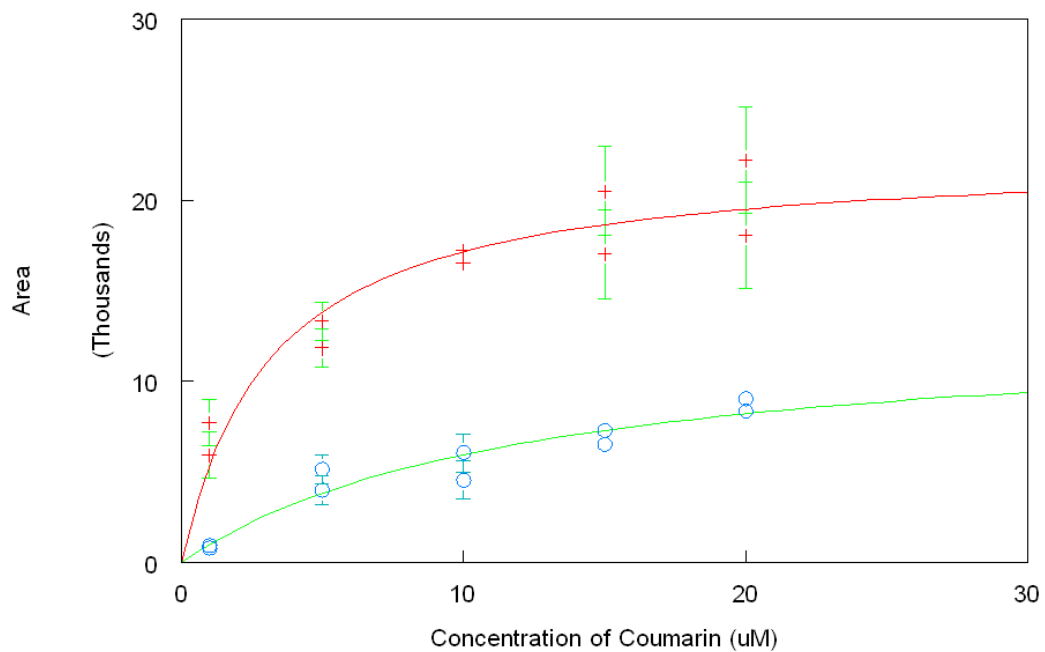


Figure III. 12: Plot of area vs. coumarin concentration in the presence (red) and absence (green) of trans-2-nonenal (0.125 mM). Reactions contained inhibitor, human liver microsomes, a range of substrate concentrations from 0 μM to 20 μM , and 1 mM NADPH.

Table III. 1: Values of V_{\max} and $V_{\max \text{ app}}$ from the Michaelis-Menton Plots for each aldehyde.

Aldehyde	Vmax	Vmax app
Crotonaldehyde	44300	30600
Trans-2-pentenal	65300	61600
Trans-2-hexenal	54700	53900
Trans-2-octenal	68200	55100
Trans-2-nonenal	22500	13200
Trans-Cinnamaldehyde	15800	16400

Table III. 2: Calculated values for K_i , K_M , $K_{M \text{ app}}$ for each unsaturated aldehyde as listed.

Aldehyde	$K_{M \text{ app}}$ (μM)	K_M (μM)	K_i (mM)
Crotonaldehyde	2.71	2.08	0.205
Trans-2-pentenal	12.4	3.36	0.171
Trans-2-hexenal	26.8	3.45	0.0196
Trans-2-octenal	10.4	2.81	0.0278
Trans-2-nonenal	13.3	1.99	0.0327
Trans-Cinnamaldehyde	5.37	1.4	0.0214

III. B. Inductions of Phase II Drug Metabolizing Enzymes by Essential Oils and Aldehydes

To probe the effects of essential oil of cassia on phase II gene induction, HepG2 liver cells were grown in culture and treated with the obtained pure essential oil (determined by GC/MS by Birch Hill Happenings) from Birch Hill Happenings. Cells were grown according to the procedure described in the experimental section and RNA and cDNA was prepared for analysis of gene expression. Initially we tested β -actin as a control, and conditions were established for consistent amplification of a portion of these genes using RT-PCR. Once the RNA of the HepG2 cells was induced and isolated,

converted into DNA and amplified via RT-PCR, the expression levels were analyzed with gel electrophoresis.

III. B. i. RT-PCR Internal Controls: β -actin and GAPDH

The results for the internal controls, β -actin and GAPDH, in the preliminary experiment with cassia oil, is shown in **Figure III. 13**. The figure shows results of RT-PCR of these genes following the procedure described previously with annealing temperatures of 56°C and 57.5°C for β -actin and GAPDH, respectively. β -actin and GAPDH had consistent bands when increasing the concentration of cassia oil, as expected. **Figure III. 13** showed the expression of β -actin for the preliminary experiments, having the correct sized fragments of 285 bp. Lanes 1 and 2 contained control cDNA, in which the cells did not have any essential oil of cassia added to them. Lane 3 samples had 10 $\mu\text{g}/\text{mL}$ of cassia oil added to the cells. Lane 4 samples contained 20 $\mu\text{g}/\text{mL}$ cassia oil, and lane 5 contained 100 $\mu\text{g}/\text{mL}$ cassia oil. The expression of this was constant and was expected to be constant as β -actin is considered a “housekeeping” gene and one that is not inducible.

Figure III. 13 show the expression levels of GAPDH, which is another internal control. The bands showed that the samples contained consistent amounts of cDNA and at the correct size of 258 bp. Lanes 1 and 2 contained control cDNA, in which the cells did not have any cassia essential oil added to them. Lane 3 samples had 10 $\mu\text{g}/\text{mL}$ of cassia oil added to the cells. Lane 4 samples contained 20 $\mu\text{g}/\text{mL}$ cassia oil, and lane 5 contained 100 $\mu\text{g}/\text{mL}$ cassia oil. These were also expected to be constant.

III. B. ii. RT-PCR Analysis of EPHX1

RT-PCR of the EPHX1 gene was also carried out, following the procedure described previously with an annealing temperatures of 60°C. **Figure III. 13** shows the expression of EPHX for the preliminary experiments, having the correct sized fragments of 273 bp. Lanes 1 and 2 contain control cDNA, in which the cells did not have any cassia oil added to them. Lane 3 samples had 10 µg/mL of cassia oil added to the cells. Lane 4 samples contained 20 µg/mL cassia oil, and lane 5 contained 100 µg/mL cassia oil. The gel shows an increase in the expression of the EPHX1 when increasing the concentration of cassia oil.

III. B. iii. RT-PCR Analysis of HNMT

RT-PCR of the HNMT gene, following the procedure described previously with annealing temperatures of 60°C. **Figure III. 13** shows the amplified cDNA from HepG2 cells treated with cassia oil for the HNMT gene. From the Figure it can be seen that a PCR product was formed having the correct size of 219 bp. Lanes 1 and 2 contain control cDNA, in which the cells did not have any cassia oil added to them. Lane 3 samples had 10 µg/mL of cassia oil added to the cells. Lane 4 samples contained 20 µg/mL cassia oil, and lane 5 contained 100 µg/mL cassia oil. The gel shows an increase in the amplified DNA for the HNMT gene with increasing concentration of cassia oil. In particular, the increase appears to be most noticeable using the two highest doses of cassia oil, 20 µg/mL and 100 µg/mL.

III. B. iv. RT-PCR Analysis of HAT1

RT-PCR of the HAT1 gene, following the procedure described previously with annealing temperatures of 62°C. The induction of the HAT1 gene is shown in **Figure III. 13** for the preliminary experiments, where a band having the correct size of 215 bp, was observed. Lanes 1 and 2 contain control cDNA, in which the cells did not have any cassia oil added to them. Lane 3 samples had 10 µg/mL of cassia oil added to the cells. Lane 4 samples contained 20 µg/mL cassia oil, and lane 5 contained 100 µg/mL cassia oil. The gel shows inconclusive evidence for the induction of the HAT1 gene when increasing the concentration of cassia oil. For example, in lane 3 there appears to be no increase in band intensity, whereas lane 4 does have an increase. At the highest dose, however it appears to drop back to a lower intensity.

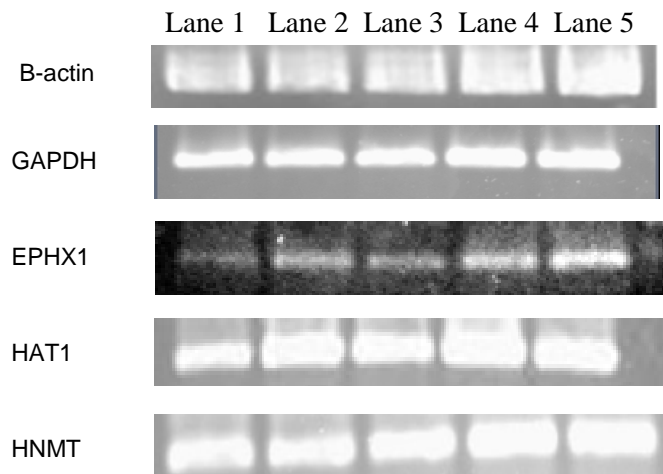


Figure III. 13: Gel electrophoresis of the β -actin gene showed a constant band for all of the samples containing, no cassia essential oil and as well as samples increasing amounts of the oil from 10 $\mu\text{g/mL}$ to 100 $\mu\text{g/mL}$.

III. B. v. RT-PCR Analysis of Heme Oxygenase-1

RT-PCR of the HO-1 gene, following the procedure described previously with annealing temperatures of 55°C. **Figure III. 14** shows the expression of HO-1 for the preliminary experiments, having the correct size of around 270 bp. Lane 1 contains control cDNA, in which the cells did not have any cassia oil added to them. Lane 2 samples had 10 $\mu\text{g/mL}$ of cassia oil added to the cells. Lane 3 samples contained 20 $\mu\text{g/mL}$ cassia oil, and lane 4 contained 100 $\mu\text{g/mL}$ cassia oil. These samples were incubated for five hours at 37°C prior to RNA isolation. The gel shows a slight increase in the amplified DNA for the HO-1 gene with increasing concentration of cassia oil,

when compared to β -actin levels. In particular, the increase appears to be most noticeable using the two middle (lane 2 and 3) doses of cassia oil, 10 $\mu\text{g/mL}$ and 20 $\mu\text{g/mL}$. There was a decrease in lane 4 which contained the highest concentration of Cassia oil, 100 $\mu\text{g/mL}$, suggesting possibly that the cells may be under-expressing this gene or perhaps even being killed.

Figure III. 15 shows the expression of HO-1 for the preliminary experiments, having the correct size of around 270 bp. Lane 1 contains control cDNA, in which the cells contained 20 $\mu\text{g/mL}$ cassia oil and were immediately harvested for RNA isolation. Lane 2 samples had 20 $\mu\text{g/mL}$ of cassia oil added and bathed at 37°C for 1 hour. Lane 3 samples contained 20 $\mu\text{g/mL}$ cassia oil added and bathed at 37°C for 5 hours. Lane 4 contained 20 $\mu\text{g/mL}$ cassia oil added and bathed at 37°C for 24 hours. The gel shows an increase in the amplified DNA for the HO-1 gene when compared to β -actin expression. In particular, the increase appears to be most noticeable using a 5 hour incubation of cassia oil (lane 3). After 24 hours of incubation the induction decreased possibly pointing to the oxidation of the aldehyde by aldehyde dehydrogenase.

Figure III. 16 shows the expression of HO-1 for the preliminary experiments in the presence of cinnamaldehyde, having the correct size of around 270 bp. Lane 1 contains control cDNA, in which the cells did not have any cinnamaldehyde added to them. Lane 2 samples had 10 $\mu\text{g/mL}$ of cinnamaldehyde added to the cells. Lane 3 samples contained 20 $\mu\text{g/mL}$ cinnamaldehyde, and lane 4 contained 100 $\mu\text{g/mL}$ cinnamaldehyde. These samples were incubated for five hours at 37°C prior to RNA isolation. The gel shows a slight increase in the amplified DNA for the HO-1 gene with

increasing concentration of cinnamaldehyde, when compared to β -actin levels. In particular, the increase appears to be most noticeable using the two middle (lane 2 and 3) doses of cinnamaldehyde, 10 $\mu\text{g/mL}$ and 20 $\mu\text{g/mL}$. However, as seen there is a slight drop in the intensity in the band of lane 4 containing the highest concentration of cinnamaldehyde (100 $\mu\text{g/mL}$), potentially due to the high increase in aldehyde concentration which could potentially harm the cells. This data is consistent with the increase in intensity of cassia oil samples in lane 2 and 3.

Figure III. 17 shows the expression of HO-1 for the preliminary experiments in the presence of cinnamaldehyde, having the correct size of around 270 bp. Lane 1 contains control cDNA, in which the cells contained 20 $\mu\text{g/mL}$ cinnamaldehyde and were immediately harvested for RNA isolation. Lane 2 samples had 20 $\mu\text{g/mL}$ of cinnamaldehyde added and bathed at 37°C for 1 hour. Lane 3 samples contained 20 $\mu\text{g/mL}$ cinnamaldehyde added and bathed at 37°C for 5 hours. Lane 4 contained 20 $\mu\text{g/mL}$ cinnamaldehyde added and bathed at 37°C for 24 hours. The gel shows an increase in the amplified DNA for the HO-1 gene when compared to β -actin expression. In particular, the increase appears to be most noticeable using a 5 hour incubation of cinnamaldehyde (lane 3). This data is consistent with the increase in intensity of cassia oil samples after five hours of incubation. With a 24 hour incubation the induction decreased pointing to the possibility of oxidation of the aldehyde.

Cassia oil consists of around 80% trans-cinnamaldehyde and in the preliminary trials seemed to have good induction on HNMT, EPHX, and HO-1. Cinnamaldehyde and cassia were both shown to also have an induction of HepG2 gene expression of the gene

Heme Oxygenase 1, a known anti-oxidant, at 20 $\mu\text{g}/\text{mL}$ and after a five hour incubation. After 24 hours of incubation the induction decreased for both cassia oil and cinnamaldehyde, possibly pointing to the oxidation of the aldehyde. The preliminary data showing this induction of these genes is consistent with past research showing electrophiles are responsible for increasing induction of antioxidant genes by the Nrf2 pathway.

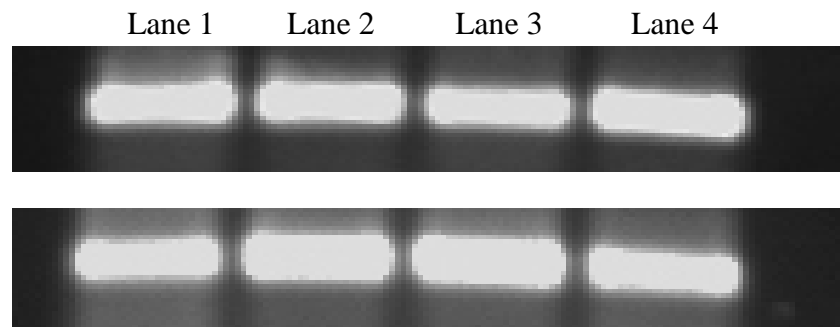


Figure III. 14: Gel Electrophoresis of the induction of the HO-1 gene in HepG2 cells, in the presence of increasing concentrations of cassia essential oil from 10 $\mu\text{g}/\text{mL}$ to 100 $\mu\text{g}/\text{mL}$, with a five hour incubation at 37°C.

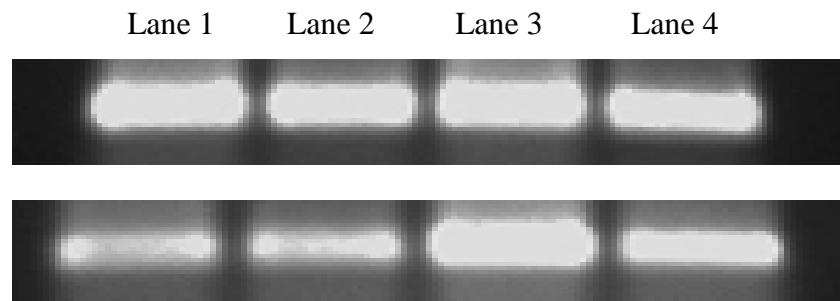


Figure III. 15: Gel Electrophoresis of the induction of the HO-1 gene in HepG2 cells, in the presence of 20 $\mu\text{g}/\text{mL}$ cassia oil for 0, 1, 6, and 24 hours of incubation at 37°C.

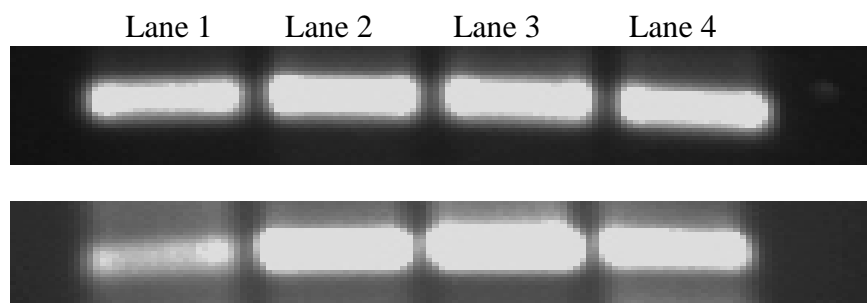


Figure III. 16: Gel Electrophoresis of the induction of the HO-1 gene in HepG2 cells, in the presence of increasing concentrations of cinnamaldehyde from 10 $\mu\text{g}/\text{mL}$ to 100 $\mu\text{g}/\text{mL}$, with a five hour incubation at 37°C.

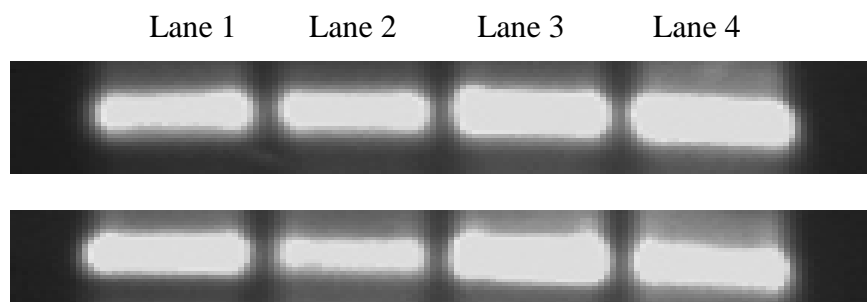


Figure III. 17: Gel Electrophoresis of the induction of the HO-1 gene in HepG2 cells, in the presence of 20 $\mu\text{g}/\text{mL}$ cinnamaldehyde for 0, 1, 6, and 24 hours of incubation at 37°C.

CHAPTER IV

CONCLUSIONS

Coumarin 7-hydroxylation assay has become a valuable tool to probe the affect of CYP2A6 in the presence of an aldehyde. Unsaturated aldehydes have been shown to have inhibited CYP2A6 with K_I values in the μM range. As predicted the unsaturated aldehydes with a carbon chain length of six to eight carbons, were strong competitors in the active site against coumarin. It has been shown that trans-cinnamaldehyde was also a good inhibitor as well.

These inhibition abilities of the unsaturated aldehydes are attributed to the active site cavity and the amino acid residues which are available for interaction with the substrate or inhibitor. Due to the presence of Asn 297, and Phe 107, the unsaturated aldehydes were able to have π stacking interactions with Phe 107 and H-bond with Asn 297. Whereas, saturated aldehydes lack the ability for π stacking interactions making it less energetically favorable to be in the active site than coumarin. This will lead to further research involving similar compounds that may be used for more potent inhibition of CYP2A6 for possible medical uses.

Electrophiles are very well known inducers of the phase II enzymes and are involved in the release of Nrf2 from the Keap1/Cul3 complex. It has now been shown that cassia oil, containing 80% trans-cinnamaldehyde induces phase II enzymes, such as Heme Oxygenase1, Epoxide Hydrolases and Histamine N-methyl-transferases and has

the potential to induce others. Cinnamaldehyde and cassia were both shown to also have an induction of HepG2 gene expression of the gene Heme Oxygenase 1, a known anti-oxidant gene, at 20 $\mu\text{g/mL}$ and after a five hour incubation. This will provide a starting point for testing this theory using other aldehydes and will lead further understanding of the Nrf2 pathway and the antioxidant defense system.

Phase I and phase II enzyme regulation has been shown with these unsaturated aldehydes and further research with such compounds would lead to further knowledge on their impacts metabolism, pharmacodynamics, and drug-drug interactions that these compounds may have.

REFERENCES

1. Valko, Marian, D. Leibfritz, J. Moncol, M. Cronin, M. Mazur, J. Telser. *The International Journal of Biochem. And Cell Biology*. **2007**, 39, 44-84.
2. Venugopal, R., Jaiswal, A. K. *Oncogene*. **1998**. 17, 3145–3156.
3. Xu, C., Li, C. Y-T., Kong, A-N. T., *Arch. Pharm. Res.* **2005**, 28, 249.
4. Ortiz de Montelleno, P. R. Cytochrome P450: Structure, Mechanism, and Biochemistry. **2005**, 3rd ed.
5. Pelkonen, O., Rautio, A., Raunio, H., Pasanen, M., *Toxicology*, **2000**, 144, 139-147.
6. Rushmore, T. H., Kong, A.-N. T., *Curr. Drug Metabolism*. **2002**, 3, 481.
7. Nakata, K., Tanaka, Y., Nakano, T., Adachi, T., Tanaka, H., Kaminuma, T., Ishikawa, T., *Drug Metab. Pharmacokinet.* **2006**, 21, 437.
8. Raunio, H., Rautio, A., Gullstén, H., and Pelkonen, O., *Br. J. Clin. Pharmacol.* **2001**, 52, 357.
9. Sansen, S., Hsu, M., Stout, C. D., Johnson, E. F., *Archives of Biochem. and Biophysics*. **2007**, 464, 197.
10. Yano, J. K., Hsu, M. Griffin, K. J., Stout, C. D., Johnson, E. F., *Nature Structural & Molecular Biology*, **2005**, 12, 822.
11. Miles, J. S., McLaren, A.W., Forrester, L. M., Glancey, M. J., Lang, M. A., Wolf, C. R., *Biochem. J.* **1990**, 267, 365.
12. Messina, E. S., Tyndale, R. F., Sellers, E. M., *J. of Pharmacology and Experimental Therapeutics*. **1997**, 282, 1608.
13. Raner, G. M., Chiang, E. W., Vaz, A. D. N., Coon, M. J., *Biochem.* **1997**, 36, 4895.
14. HonGen, W., JianZhong, H., ShiZhong, C., TieMin, A., *Chinese J. of Info. On Trad. Chinese Med.* **2002**, 9, 42.
15. Creaven, P. J., Parke, D. V., Williams, R. T. *Biochem. J.* **1965**, 96, 390.

16. Prestera, T., Talalay, P., *Proc. Natl. Acad. Sci.* **1995**, 92, 8965.
17. Rachakonda, G., Xiong Y., Sekhar K., Stamer, D., Liebler, D., Freeman, M. *Chem. Res. Toxicol.* 2008. 21(3), 705–710.
18. Hong, F., Sekhar, K. R., Freeman, M. L., Liebler, D. C. *J. Biol. Chem.* 2005. 280, 31768–31775.
19. Kobayashi, M.; Yamamoto, M. *Antioxid. Redox Signal.* 2005. 7, 385–394.
20. Shin-Pei Yang; Wilson, K.; Kawa, A.; Raner, G. M.; *Food and Chemical Toxicology.* 2006. 44. 1075-1081.
21. Lyn-Cook, B. D., Yan-Sanders, Y., Moore, S., Taylor, S., Word, B., Hammons, G. J., *Cell Biol. Toxicol.* **2006**, 22, 73.
22. Kutty, R. K., Kutty, G., Nagineni, C. N., Hooks, J. J., Chader, G. J., Wiggert, B., *Annals New York Acad. of Sci.* **1992**, 428.
23. Westerink, W. M. A., Schoonen, W. G. E. J., *Toxicology in Vitro.* **2007**, 21, 1592.
24. Waxman, D. J., Chang, T. K. H., *Methods in Molecular Biol.* **1998**, 107, 111.
25. Kamataki, T., Fujita, K., Nakayama, K., Yamazaki, Y., Miyamoto, M., Ariyoshi, N. *Drug Metab. Rev.* **2002**, 34, 667.